Universidade de Aveiro Departamento de Física
2010

Alexandre Miguel de Araújo Lopes

Electronic, thermodynamic and transport properties of the diamond chain

Alexandre Miguel de Araújo Lopes

Electronic, thermodynamic and transport properties of the diamond chain

Dissertação apresentada à Universidade de Aveiro para cumprimento dos requisitos necessários à obtenção do grau de Mestre em Física, realizada sob a orientação científica do Professor Doutor Ricardo Assis Guimarães Dias, Professor auxiliar do Departamento de Física da Universidade de Aveiro

I dedicate this work to my parents, my brother and my girlfriend, Filipa

o júri / the jury

presidente / president

Prof. Dr. Armando José Trindade das Neves
Professor associado da Universidade de Aveiro

Prof. Dr. Ricardo Assis Guimarães Dias
Professor auxiliar da Universidade de Aveiro

Prof. Dr. Luís Miguel Fortuna Rodrigues Martelo
Professor auxiliar da Faculdade de Engenharia da Universidade do Porto

agradecimentos / acknowledgements

I would like to thank my advisor for all the support given and because he is the best advisor one could have.

I would also like to give a special thanks to my parents, my brother and my girlfriend, Filipa, for having the patience to endure those little moments when I was probably so annoying.

Resumo

No presente trabalho estudamos as propriedades electrónicas e de transporte da cadeia de diamantes quando esta é penetrada por um fluxo magnético. Não só estudamos a cadeia perfeita como também o efeito de acoplamento entre segundos vizinhos, da introdução de impurezas no sistema e de interacções. Demonstramos que o sistema exibe propriedades muito interessantes como bandas *flat* controláveis por fluxo magnético, partículas de Dirac, um comportamento isolador-semicondutor controlável por fluxo magnético e um rico diagrama de fases em MF. As potenciais applicações científicas e tecnológicas do referido sistema são muitas, desde o estudo de modelos de acoplamento forte (*strong coupling*), à construção de portas lógicas e de sistemas de informação quântica.

Abstract

We study the electronic and transport properties of the diamond chain when this is threaded by a magnetic field. We address not only the perfect chain but we also study the effect of next nearest neighbors coupling, of introducing impurities in the system and of interactions. The system is shown to exhibit many interesting properties like magnetic flux controlled flat bands, Dirac like particles, a magnetic flux tuned insulating-semiconducting behavior and very rich MF phase transitions. The potential scientific and technological applications of such systems are many, ranging from the study of strong coupling models to the construction of logic gates and quantum information systems.

Contents

1 Introduction **1**
- 1.1 Introduction . . . 1
- 1.2 The tight binding approximation . . . 1
- 1.3 Quantum rings and the AB effect . . . 3

2 Energy spectrum of the diamond chain **5**
- 2.1 The simple Diamond chain . . . 5
  - 2.1.1 Zero flux . . . 7
  - 2.1.2 Half flux quantum per diamond . . . 8
  - 2.1.3 General ϕ . . . 10

3 Electronic and thermodynamic properties of the diamond chain **14**
- 3.1 Density of states . . . 14
- 3.2 Persistent currents . . . 15
- 3.3 Group velocity and effective mass . . . 16
- 3.4 Dependence of the filling on the Fermi energy . . . 17
- 3.5 Ground state energy . . . 18
- 3.6 Thermodynamics . . . 19

4 Diamond star and connecting the diamond **21**
- 4.1 Diamond star . . . 21
- 4.2 Connecting the diamond . . . 22
  - 4.2.1 Internal hops . . . 22
  - 4.2.2 Internal and external hops . . . 23

5 Impurities and ABC diamonds **27**
- 5.1 Single localized impurity . . . 27
- 5.2 ABC Diamond . . . 33

6 Interactions in the diamond chain **36**
- 6.1 On-site Coulomb repulsion . . . 37
  - 6.1.1 Ferromagnetic ordering . . . 37
  - 6.1.2 Antiferromagnetic ordering . . . 38
- 6.2 Nearest neighbors Coulomb interaction . . . 39

7 Conductance **41**
- 7.1 Conductance in the diamond star . . . 41

A Thermodynamics of a single mode fermionic oscillator **46**

Chapter 1

Introduction

1.1 Introduction

The interest in low dimensional systems has increased recently, motivated not only by advances in production techniques but also by a better theoretical understanding of such systems associated with novel and interesting properties they exhibit. These systems range from 0D systems of which one good promissing example is the single electron transistor to 1D systems such as carbon nanotubes and 2D systems such as graphene. Graphene, first isolated in 2004[1] [2] is a hallmark of low dimensional physics and is seen as an excellent candidate for the future of electronics given its peculiar properties such as massless charge carriers, extremely high mobilities even at room temperature, [3] and its ability to show the quantum hall effect at room temperature. [4] We should note that despite the fact that its 3D counterpart, graphite, is comprised of weakly interacting sheets of graphene, it does not exhibit such phenomena. We have come a long way since Landau and Peierls theorized that free standing 2D crystals should not exist! [5, 6]

In the present text we will study the electronic and transport properties of quasi one dimensional systems consisting of an array of quantum rings - bipartite lozenge chains. Quantum rings due to their topology are capable of exhibiting the Aharonov-Bohm effect, a purely quantum mechanical effect related with gauge invariance, when threaded by a magnetic flux. Here we will simply call these bipartite lozenge chains diamond chains, due to their topology (note that it has nothing to do with carbon made diamond). We will start by introducing the concepts of tight binding approximation and the Aharonov-Bohm effect (AB effect). We will then study the electronic spectrum of our diamond chain using a simple nearest neighbors tight binding description followed by a thermodynamical analysis of the system. We also consider tunneling between second neighbors in more than one fashion and compare with previous results. We proceed to study the physical effects of adding disorder to our system. Finally we add interactions to our system, treating them using mean field approximation, and we also study the conductance of our system when weakly coupled to external leads.

1.2 The tight binding approximation

The tight binding approximation is a very useful approximation used to calculate the band structure of materials and offers in many cases an improvement over the free electron picture. [7] Despite the fact that it does not contemplates interactions, these are easily introduced into a tight binding Hamiltonian.

Let us consider a system with exactly one atom per lattice point (it does not matter if our lattice is 1D, 2D or 3D). Its Hamiltonian, neglecting interactions, is given by,

$$H = \sum_{\vec{R}} H_a\left(\vec{R}\right), \tag{1.1}$$

where $\vec{R}$ is a Bravais vector and $H_a(\vec{R})$ is the Hamiltonian of the atom at point $\vec{R}$.

[1] There is some controversy regarding the discovery of isolated graphene since it appears to have been isolated before Geim's team in 2004. It is however indisputable that Geim's team discovery opened up the golden age of graphene. [1]

The tight binding approximation consists in assuming that in the vicinity of a lattice point the full Hamiltonian of the system is well approximated by the Hamiltonian of the corresponding atom,

$$H = H_a + \Delta H, \tag{1.2}$$

where H_a is the Hamiltonian of an atom located in origin and $\Delta H = \sum_{\vec{R}\neq 0} H_a\left(\vec{R}\right)$ is the correction needed to reproduce the full Hamiltonian, which we expect to be small near the origin.

The eigenvectors of the atomic Hamiltonian are obviously the atomic wavefunctions $|\phi\rangle$. These wavefunctions would be wavefunctions of the whole crystal Hamiltonian, provided the wavefunction of an atom at point $(\vec{R}_i)$ satisfied,

$$\phi(\vec{R}_i + \vec{r}) \to 0, \quad ||\vec{r}|| \to ||\vec{R}_i - \vec{R}_j||, \tag{1.3}$$

where $\vec{R}_j$ is the position of its neighbors. That is, the atomic wavefunctions would be eigenfunctions of the crystal Hamiltonian if the overlap of wavefunctions of different atoms was zero, i.e., if they were orthogonal.

We require then, in order to have ΔH small near our atom located at the origin and for the tight binding approximation to be a good one, that,

$$\phi(\vec{R} + \vec{r}) \approx 0, \quad ||\vec{r}|| \approx ||\vec{R} - \vec{R}'||, \tag{1.4}$$

i.e., we require the overlap of the wavefunction of different atoms to be as small as possible. If it is not, then our tight binding approximation will fail.

Since our system is translational invariant we know that its eigenfunctions are Bloch functions. Expanding the Bloch function in a basis of localized functions $\Phi(\vec{R})$, called Wannier functions, located at lattice points $\vec{R}$ we have,

$$\left|\psi_{\vec{k}}\right\rangle = \sum_{\vec{R},n} \mathrm{e}^{\mathrm{i}\vec{k}\cdot\vec{R}} \left|\Phi(\vec{R})\right\rangle_n, \tag{1.5}$$

where n is the band index.

Just as the Bloch function describes a delocalized electron with definite momentum, a Wannier function describes a localized electron with no definite momentum. If our tight binding approximation is justified then the Wannier functions will be identical to the atomic wavefunctions. In a one dimensional case, Eq. (1.5) can be written in second quantization formalism as,

$$c_k^\dagger \left|0\right\rangle = \sum_j \mathrm{e}^{\mathrm{i}kja} c_j^\dagger \left|0\right\rangle, \tag{1.6}$$

where $c_k^\dagger$ creates an electron with momentum k, a Bloch electron, and $c_j^\dagger$ creates an electron in a Wannier state at position $r = aj$. From now on we will assume, without any loss of generality that, $a = 1$. We will also assume that only a single atomic orbital is important for the transport properties of the system.

We can write the Hamiltonian of our system as,

$$H = \sum_{\vec{R}} H_W(\vec{R}) + \Delta H', \tag{1.7}$$

where $H_W(\vec{R})$ is a Wannier Hamiltonian centered on $\vec{R}$ whose eigenvalues are Wannier functions centered on $\vec{R}$ and $\Delta H'$ is the correction needed to reproduce the full crystal Hamiltonian (since the Wannier Hamiltonians are not exactly the atomic ones).

Let us define,

$$\left\langle 0\right| c_i \Delta H' c_j^\dagger \left|0\right\rangle = -t_{i,j} = \int \Phi(R_i - r)^* \Delta H' \Phi(R_j - r)\mathrm{d}r, \tag{1.8}$$

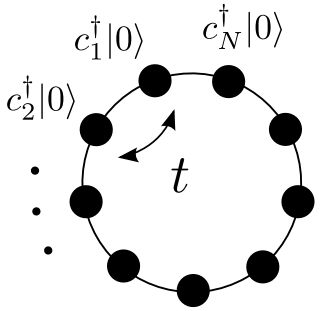

Figure 1.1: A tight-binding quantum ring.

for the matrix elements of $\Delta H'$ on the Wannier basis. We can then write the Hamiltonian of our system as,

$$H = \sum_j \epsilon_j c_j^\dagger c_j - \sum_{i,j,i\neq j} t_{i,j} \left(c_i^\dagger c_j + c_j^\dagger c_i \right), \tag{1.9}$$

where

$$\epsilon_j = \langle 0 | \, c_j H c_j^\dagger \, | 0 \rangle = \int \Phi(R_j)^* H \Phi(R_j) \mathrm{d}r, \tag{1.10}$$

is the on-site energy of site j.

If we take only the overlap between nearest neighbor atomic wavefunctions to be non zero the perturbation only couples nearest neighbor Wannier functions and we have,

$$t_{i,j} = \delta_{i,j} t, \tag{1.11}$$

where we have also assumed the isotropy of our system. Considering also that the on-site energy is site independent,

$$\epsilon_j = \epsilon_0, \forall j, \tag{1.12}$$

we can write,

$$H = \epsilon_0 \sum_j c_j^\dagger c_j - t \sum_j c_{j+1}^\dagger c_j + c_j^\dagger c_{j+1}. \tag{1.13}$$

Through the rest of the text when we mention the tight binding model we will assume the above Hamiltonian unless otherwise specified.

In the present context we can interpret the overlap integral t as the probability of an electron hoping between nearest neighbor sites and for this reason it is called *hoping amplitude*.

1.3 Quantum rings and the AB effect

Let us consider translational symmetric quantum ring consiting of N sites as depicted in Fig. 1.1. Using the tight binding approximation its Hamiltonian can be written as,

$$H = -t \sum_{j=1}^{N} c_{j+1}^\dagger c_j + c_j^\dagger c_{j+1}. \tag{1.14}$$

By transforming the operators into Fourier/momentum space,

$$c_k^\dagger = \sum_j \mathrm{e}^{\mathrm{i}kj} c_j^\dagger, \tag{1.15}$$

and using the orthogonality relation (valid for periodic boundary conditions),

$$\sum_j \mathrm{e}^{\mathrm{i}j(k-q)} = \delta_{k,q} N, \tag{1.16}$$

the Hamiltonian is diagonalized. Its eigenvalues are given by,

$$\epsilon_k = -2t\cos(k), \quad k = \frac{2\pi n}{N}, \tag{1.17}$$

where,

$$n = \begin{cases} -\frac{N}{2}, -\frac{N}{2}+1, \cdots, \frac{N}{2}-1 & , N \text{ even} \\ -\frac{N-1}{2}, -\frac{N-1}{2}+1, \cdots, \frac{N-1}{2} & , N \text{ odd} \end{cases} \tag{1.18}$$

so that k belongs to the first Brillouin zone (FBZ).

Let us now introduce a magnetic flux through the ring and perpendicular to it. Let us also consider that the flux pierces a region where the amplitude of the system's wavefunction is almost zero. Since the probability of an electron encountering the magnetic flux is basically zero, one could argue, on classical grounds, that since no force is exerted on the electrons nothing happens. However, as demonstrated by Ehrenberg and Siday and latter by Aharonov and Bohm, [8, 9] the requirement of gauge invariance implies that the phase of the wavefunction of an electron circulating through the ring is affected and therefore, altough no magnetic field acts directly on the system, its properties are in fact affected by the magnetic flux. This is a simple consequence of the non locality of quantum mechanics. The wavefunction of the electron when the ring is threaded by the magnetic flux, $\psi_B(\theta)$, is related to its wavefunction in zero field, $\psi_0(\theta)$, by,

$$\psi_B(\theta) = \exp\left[\mathrm{i}\frac{q}{\hbar}\int \vec{A}\cdot \mathrm{d}\vec{l}\right]\psi_0(\theta), \tag{1.19}$$

where θ is the angular position on the ring. Assuming a solenoidal like field inside our ring, perpendicular to its plane, implies that after a loop, the wavefunction of the electron is,

$$\psi_B(2\pi) = \psi_B(0)\mathrm{e}^{\mathrm{i}\theta\phi/\phi_0}, \tag{1.20}$$

where $\phi_0 = h/q$ is the quantum of flux. From now on we will make $2\pi\phi/\phi_0 \to \phi$, where ϕ is now the reduced flux. Therefore, if the electron loops around the ring once, its wavefunction must acquire a phase given by the reduced flux. This can be inserted in our tight binding Hamiltonian by using the so called *twisted boundary conditions*,

$$H = -t\sum_{j=1}^{N-1}\left(c_{j+1}^\dagger c_j + c_j^\dagger c_{j+1}\right) - t\left(\mathrm{e}^{\mathrm{i}\phi}c_N^\dagger c_1 + \mathrm{e}^{-\mathrm{i}\phi}c_1^\dagger c_N\right). \tag{1.21}$$

Performing the gauge transformation,

$$c_j^\dagger \to \mathrm{e}^{-\mathrm{i}\phi/Nj}c_j^\dagger \tag{1.22}$$

our Hamiltonian can be written in the translational invariant form,

$$H = -t\sum_j \mathrm{e}^{\mathrm{i}\phi/N}c_{j+1}^\dagger c_j + \mathrm{e}^{-\mathrm{i}\phi/N}c_j^\dagger c_{j+1}, \tag{1.23}$$

where the flux has now been spread equally thoughout all hops. As before, due to its translational invariance, the Hamiltonian is immediately diagonalized by transforming it into Fourier space, its one particle eigenvectors being given by,

$$c_k^\dagger|0\rangle = \sum_j \mathrm{e}^{\mathrm{i}kj}c_j^\dagger|0\rangle, \tag{1.24}$$

and the associated eigenvalues being,

$$\epsilon_k = -2t\cos\left(k - \frac{\phi}{N}\right). \tag{1.25}$$

Chapter 2

Energy spectrum of the diamond chain

In this chapter we will study the spectrum and thermodynamic properties of a diamond chain threaded by a magnetic flux using a tight binding approach. We will begin by numerically studying finite systems using periodic boundary conditions (which will always be employed throughout this text) and see the dependence of the single particle eigenvalues on the flux. We then study analytically the particular cases of zero flux, $\phi = 0$ and half quantum flux per diamond, $\phi = \pi$, introducing a particular transformation which we then generalize to an arbitrary value of flux. As will be seen, this model shows the very peculiar characteristic of having a completely flat band on the middle of its spectrum for general ϕ and for $\phi = \pi$, all of its bands become flat. We also note that although this system is well studied in the absence of flux, [10–12] the bibliography for the situation with flux is very scarce [13] and we derive interesting new results.

2.1 The simple Diamond chain

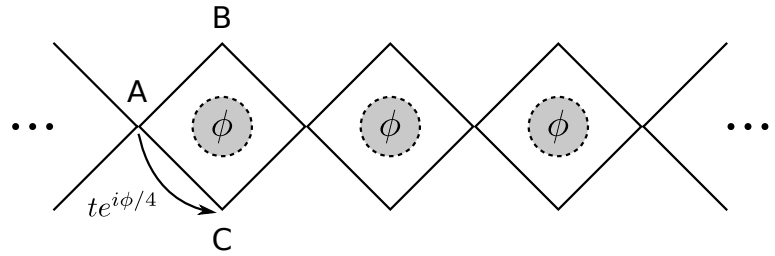

Figure 2.1: The diamond chain tight binding model.

Let us consider a system consisting of a repeating pattern of sites, ABC, where the sites B and C are nearest-neighbors of the A sites. If we consider that the sites are equal and equidistant,[1], we will have a chain of diamonds-like geometry. Let us also introduce a magnetic flux on the interior of the diamonds, with the respective Peierls phase equally distributed throughout the four sites comprising a single ring. We then have the system depicted in Fig. 2.1, which we will call diamond chain. Such system can be used to model ML_2 (metal-ligand) chains, [14] azurite [15] and can be generalized to molecular systems displaying similar topology. Also, given nowadays nanofabrication techniques, such as electron beam lithography, a diamond chain like system can in principle be built from scratch.

Neglecting interactions and using a nearest-neighbors tight binding approach we arrive at the following Hamiltonian for the system,

$$H = -t \sum_{j}^{N_c} A_j^\dagger \left(\mathrm{e}^{\mathrm{i}\phi/4} B_j + \mathrm{e}^{-\mathrm{i}\phi/4} C_j \right) + A_{j+1}^\dagger \left(\mathrm{e}^{-\mathrm{i}\phi/4} B_j + \mathrm{e}^{\mathrm{i}\phi/4} C_j \right) + \mathrm{h.c.}. \tag{2.1}$$

[1] We only require this so that the overlap integral and the on-site energy are constant.

Diagonaling the Hamiltonian for a finite number of sites, and for a single particle system[2], the following results can summarized,

- The Hamiltonian has a flat band for $\epsilon_k = 0$ which is also flux independent;
- For an even number of unit cells N_c and for $\phi = 0$, the flux dependent eigenvalues do not cross the zero energy level while they do for an odd number of unit cells;
- For $\phi = \pi$ the system is highly degenerate and presents only three levels. As a consequence the density of states (DOS) is singular in this situation;
- For $N_c = 4n$ with n integer two flux independent energies appear for $\epsilon_k = \pm 2t$. Since the derivative of the energy in order to the flux is zero for these bands they do not give rise to persistent currents;
- The system is periodic on the flux with period $\phi = 2\pi$ when N_c is even and with period $\phi = 4\pi$ when N_c is odd. This difference is only relevant for small systems and as expected its period tends to 2π for very large systems;
- For $\phi = 2\pi$ the flux dependent eigenvalues cross the dispersionless band independently on the parity of N_c.

The eigenvalues as a function of the flux, for several number of unit cells, are represented in Fig. 2.2.

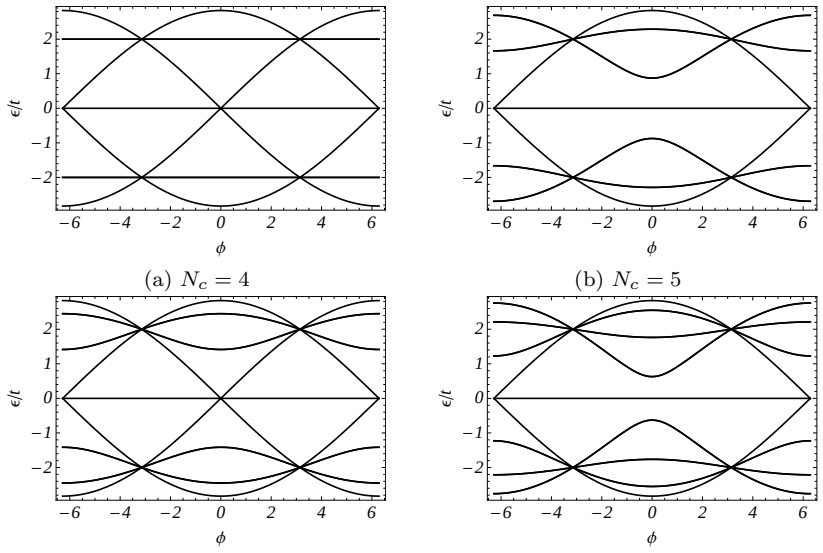

(a) $N_c = 4$ (b) $N_c = 5$

(c) $N_c = 6$ (d) $N_c = 7$

Figure 2.2: One particle eigenvalues dependence on the flux for different number of unit cells. Note the flat flux bands for $\epsilon_k = \pm 2$ for $N_c = 4$. These bands can be found whenever the number of unit cells is a multiple of four. Note also that when N_c is even, the flux dependent eigenvalues do not intercept the origin, while they do for odd N_c.

Some of the symmetries of this system are:

- *Translational* symmetry, i.e., the Hamiltonian is invariant under the operation,

[2]Since there are no interactions the full information of the system can be obtained by diagonalizing the Hamiltonian in a single particle space

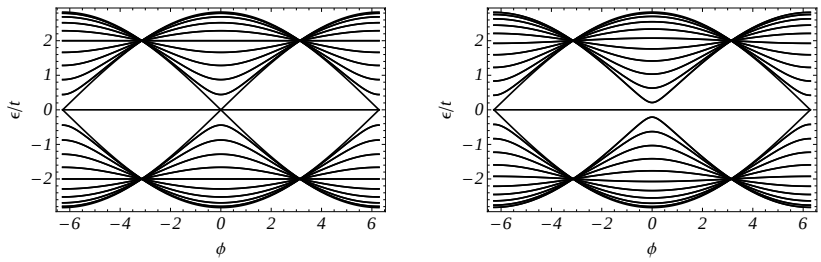

(a) $N_c = 20$ (b) $N_c = 21$

Figure 2.3: One particle eigenvalues dependence on the flux comparison for an even and an odd number of cells, for a large system. Note that the difference between the odd and the even situation is not very large (generally speaking), and goes to zero when the size of the system becomes infinite

$$\begin{Bmatrix} A_j^\dagger \\ B_j^\dagger \\ C_j^\dagger \end{Bmatrix} \to \begin{Bmatrix} A_i^\dagger \\ B_i^\dagger \\ C_i^\dagger \end{Bmatrix}, \quad \forall j, i \tag{2.2}$$

- *BC permutation-flux symmetrization* symmetry, i.e., the Hamiltonian is invariant under the operation,

$$\begin{Bmatrix} B_j^\dagger \\ C_j^\dagger \\ \phi \end{Bmatrix} \to \begin{Bmatrix} C_j^\dagger \\ B_j^\dagger \\ -\phi \end{Bmatrix}, \quad \forall j \tag{2.3}$$

We start by studying the simpler particular situations, $\phi = 0$ and $\phi = \pi$.

2.1.1 Zero flux

In this situation the Hamiltonian reduces to,

$$H = -t \sum_j \left(B_j^\dagger + C_j^\dagger \right) (A_j + A_{j+1}) + \text{h.c.}. \tag{2.4}$$

As can be seen, the B and C sites are equivalent, a symmetry that is broken by a finite flux.

Let us define bonding/symmetric and anti-bonding/anti-symmetric operators that correspond to a rotation of the creation/annihilation operators on sites B and C,

$$\begin{aligned} b_j^\dagger &= \frac{1}{\sqrt{2}} \left(B_j^\dagger + C_j^\dagger \right), \\ a_j^\dagger &= \frac{1}{\sqrt{2}} \left(B_j^\dagger - C_j^\dagger \right). \end{aligned} \tag{2.5}$$

Inserting the new operators on the Hamiltonian we have,

$$H = -\sqrt{2}t \sum_j^{N_c} A_j^\dagger b_j + b_j^\dagger A_j + b_j^\dagger A_{j+1} + A_{j+1}^\dagger b_j, \tag{2.6}$$

and trivially,

$$H a_j^\dagger |0\rangle = 0. \tag{2.7}$$

Therefore the states $a_j^\dagger |0\rangle$ correspond to localized, dispersionless eigenstates of the system. Our Hamiltonian is now that of a dimerized chain, as depicted in Fig. 2.4.

Transforming our Hamiltonian into Fourier space we have,

$$H = -2\sqrt{2}t \sum_k \mathrm{e}^{-\mathrm{i}k/2} \cos(k/2) A_k^\dagger b_k + \text{h.c.}, \tag{2.8}$$

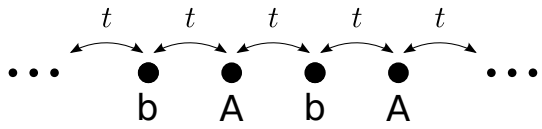

Figure 2.4: Ab chain.

which is a block diagonal Hamiltonian in the basis $\left\{b_k^\dagger, A_k^\dagger\right\}_k |0\rangle$ [3], being the direct sum of N_c blocks, $H = \oplus_k H_k$. The restriction of the Hamiltonian to the subspace $\left\{b_k^\dagger, A_k^\dagger\right\}_k |0\rangle$, i.e., the block H_k is,

$$H_k = -2\sqrt{2}t \begin{pmatrix} 0 & \mathrm{e}^{-\mathrm{i}k/2}\cos(k/2) \\ \mathrm{e}^{\mathrm{i}k/2}\cos(k/2) & 0 \end{pmatrix}. \tag{2.9}$$

Diagonalizing the above matrix, we find that the Hamiltonian of the Ab chain can be written as,

$$H = \sum_k \epsilon_k (f_k^\dagger f_k - d_k^\dagger d_k), \tag{2.10}$$

where,

$$\epsilon_k = 2\sqrt{2}t\cos(k/2), \tag{2.11}$$

and where the operators

$$\begin{aligned} d_k^\dagger &= \frac{1}{\sqrt{2}}\left(\mathrm{e}^{-\mathrm{i}k/4}A_k^\dagger + \mathrm{e}^{\mathrm{i}k/4}b_k^\dagger\right), \\ f_k^\dagger &= \frac{1}{\sqrt{2}}\left(\mathrm{e}^{-\mathrm{i}k/4}A_k^\dagger - \mathrm{e}^{\mathrm{i}k/4}b_k^\dagger\right), \end{aligned} \tag{2.12}$$

create an electron with momentum k on the lower and upper band respectively (see Fig. 2.5)

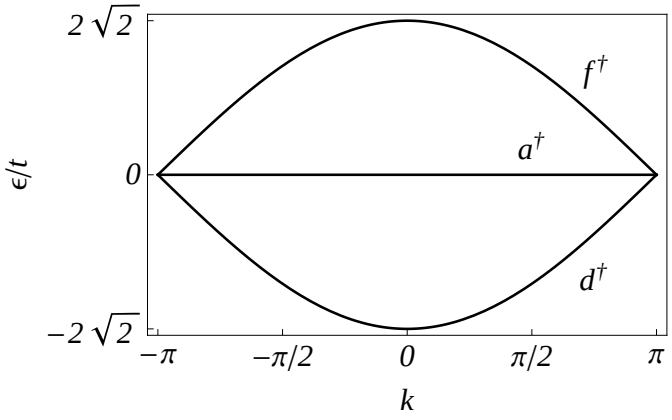

Figure 2.5: Dispersion relation for $\phi = 0$. We have a three band system, the bottom (d) and top bands (f) being dispersive and symmetric about middle band (a) which is a flat (dispersionless) band. Note that these bands intercept for $k = -\pi$.

2.1.2 Half flux quantum per diamond

For $\phi = \pi$, which corresponds to a flux of half flux quantum, the Hamiltonian becomes,

$$H = -t\sum_j \left(\mathrm{e}^{-\mathrm{i}\pi/4}B_j^\dagger + \mathrm{e}^{\mathrm{i}\pi/4}C_j^\dagger\right)A_j + \left(\mathrm{e}^{\mathrm{i}\pi/4}B_j^\dagger + \mathrm{e}^{-\mathrm{i}\pi/4}C_j^\dagger\right)A_{j+1} + \text{h.c.}. \tag{2.13}$$

[3] We are only considering a single particle Hilbert space since we have no interactions.

Let us define the rotated operators,

$$\begin{aligned} b_j^\dagger &= \frac{1}{\sqrt{2}}\left(\mathrm{e}^{-\mathrm{i}\pi/4}B_j^\dagger + \mathrm{e}^{\mathrm{i}\pi/4}C_j^\dagger\right), \\ c_j^\dagger &= \frac{1}{\sqrt{2}}\left(\mathrm{e}^{\mathrm{i}\pi/4}B_j^\dagger + \mathrm{e}^{-\mathrm{i}\pi/4}C_j^\dagger\right). \end{aligned} \tag{2.14}$$

Substituting in the Hamiltonian gives us,

$$H = -\sqrt{2}t\sum_j A_j^\dagger b_j + b_j^\dagger A_j + A_{j+1}c_j + c_j^\dagger A_{j+1}. \tag{2.15}$$

This is the direct sum of N_c independent Hamiltonians of a three sites tight binding model with open boundary conditions, as depicted in Fig. 2.6. It is then obvious that we are able to find a localized eigenbasis for the Hamiltonian. It also implies that transport is forbidden for this specific value of magnetic flux.

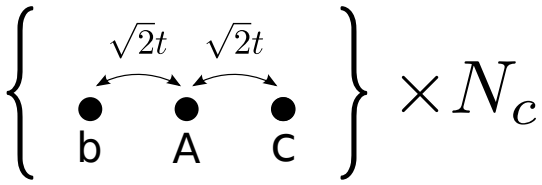

Figure 2.6: For half flux quantum the diamond Hamiltonian can be mapped into the Hamiltonian of N_c independent three sites system.

The Hamiltonian is diagonalized by the transformations,

$$\begin{aligned} d_j^\dagger &= \frac{1}{2}\left(c_{j-1}^\dagger + \sqrt{2}A_j^\dagger + b_j^\dagger\right), \\ a_j^\dagger &= \frac{1}{\sqrt{2}}\left(c_{j-1}^\dagger - b_j^\dagger\right), \\ f_j^\dagger &= \frac{1}{2}\left(c_{j-1}^\dagger - \sqrt{2}A_j^\dagger + b_j^\dagger\right), \end{aligned} \tag{2.16}$$

and can be written as,

$$H = \epsilon_+ \sum_j^{N_c} f_j^\dagger f_j - d_j^\dagger d_j, \tag{2.17}$$

where,

$$\epsilon_+ = 2t. \tag{2.18}$$

The system therefore, only has three N_c times degenerate (single particle) eigenvalues, that are independent of the momentum (flat bands),

$$\epsilon = 0, \pm 2t, \tag{2.19}$$

as depicted in Fig. 2.7.

The transformation equations given in Eq. 2.16 can be written, in the real space as,

$$\begin{aligned} d_j^\dagger &= \frac{1}{\sqrt{2}}A_j^\dagger + \frac{1}{2\sqrt{2}}\left(\mathrm{e}^{\mathrm{i}\pi/4}B_{j-1}^\dagger + \mathrm{e}^{-\mathrm{i}\pi/4}C_{j-1}^\dagger + \mathrm{e}^{-\mathrm{i}\pi/4}B_j^\dagger + \mathrm{e}^{\mathrm{i}\pi/4}C_j^\dagger\right), \\ a_j^\dagger &= \frac{1}{2}\left(\mathrm{e}^{\mathrm{i}\pi/4}B_{j-1}^\dagger + \mathrm{e}^{-\mathrm{i}\pi/4}C_{j-1}^\dagger - \mathrm{e}^{-\mathrm{i}\pi/4}B_j^\dagger - \mathrm{e}^{\mathrm{i}\pi/4}C_j^\dagger\right), \\ f_j^\dagger &= -\frac{1}{\sqrt{2}}A_j^\dagger + \frac{1}{2\sqrt{2}}\left(\mathrm{e}^{\mathrm{i}\pi/4}B_{j-1}^\dagger + \mathrm{e}^{-\mathrm{i}\pi/4}C_{j-1}^\dagger + \mathrm{e}^{-\mathrm{i}\pi/4}B_j^\dagger + \mathrm{e}^{\mathrm{i}\pi/4}C_j^\dagger\right), \end{aligned} \tag{2.20}$$

and correspond to localized eigenstates as shown in Fig. 2.8.

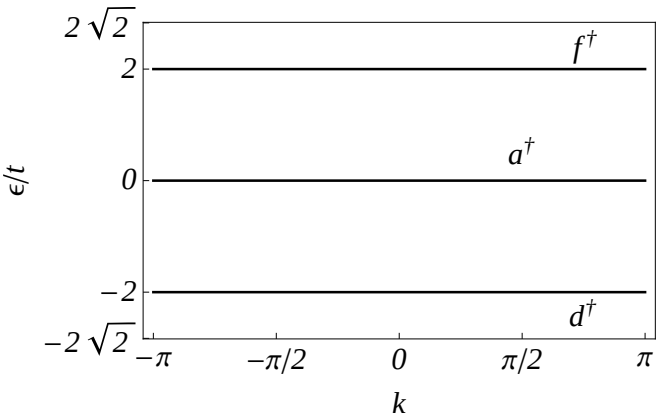

Figure 2.7: The dispersion relation for half flux quantum ($\phi = \pi$) consists simply of three N_c times degenerate flat bands with $\epsilon_k = 0, \pm 2t$.

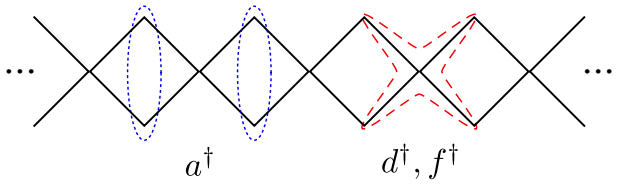

Figure 2.8: Localized eigenstates for $\phi = \pi$. Note that states $a_j^\dagger |0\rangle$ are only localized on B and C sites.

2.1.3 General ϕ

Let us now consider the case of an arbitrary flux threading the rings so that the Hamiltonian is,

$$H = -t \sum_j^{N_c} A_j^\dagger \left(\mathrm{e}^{\mathrm{i}\phi/4} B_j + \mathrm{e}^{-\mathrm{i}\phi/4} C_j \right) + A_{j+1}^\dagger \left(\mathrm{e}^{-\mathrm{i}\phi/4} B_j + \mathrm{e}^{\mathrm{i}\phi/4} C_j \right) + \mathrm{h.c.}. \tag{2.21}$$

Since this is a non-interacting Hamiltonian possessing translational invariance it can be easily diagonalized by transforming it directly into the momentum space. However, to gain some more insight into the model, let us generalize the transformation equations (2.5) and (2.14), employed for $\phi = 0$ and $\phi = \pi$. By inspection, we are led to propose,

$$\begin{aligned} b_j^\dagger &= \frac{1}{\sqrt{2}} \left(\mathrm{e}^{-\mathrm{i}\phi/4} B_j^\dagger + \mathrm{e}^{\mathrm{i}\phi/4} C_j^\dagger \right), \\ c_j^\dagger &= \frac{1}{\sqrt{2}} \left(\mathrm{e}^{\mathrm{i}\phi/4} B_j^\dagger - \mathrm{e}^{\mathrm{i}\phi} \mathrm{e}^{\mathrm{i}\phi/4} C_j^\dagger \right), \end{aligned} \tag{2.22}$$

were we have required the unitarity of the transformation, so that the canonical anti-commutation relations are preserved. Since the transformation is unitary, its inverse is easily calculated,

$$\begin{aligned} B_j^\dagger &= \frac{1}{\sqrt{2}} \left(\mathrm{e}^{\mathrm{i}\phi/4} b_j^\dagger + \mathrm{e}^{-\mathrm{i}\phi/4} c_j^\dagger \right), \\ C_j^\dagger &= \frac{1}{\sqrt{2}} \left(\mathrm{e}^{-\mathrm{i}\phi/4} b_j^\dagger - \mathrm{e}^{-\mathrm{i}3\phi/4} c_j^\dagger \right). \end{aligned} \tag{2.23}$$

Substituting in the Hamiltonian and applying the gauge transformation $c_j^\dagger \to -\mathrm{i}\mathrm{e}^{-\mathrm{i}\phi/2} c_j^\dagger$ to simplify the result, we obtain,

$$H = -t_1 \sum_j \left(b_j^\dagger A_j + \mathrm{h.c.} \right) - t_2 \sum_j \left(b_j^\dagger A_{j+1} + \mathrm{h.c.} \right) - t_3 \sum_j \left(c_j^\dagger A_{j+1} + \mathrm{h.c.} \right), \tag{2.24}$$

where,

$$\begin{aligned} t_1 &= \sqrt{2}t, \\ t_2 &= \sqrt{2}\cos(\phi/2)t, \\ t_3 &= \sqrt{2}\sin(\phi/2)t. \end{aligned} \tag{2.25}$$

The resulting system is depicted in Fig. 2.9. By setting $\phi = 0$ or $\phi = \pi$ it is easy to recover our previous results: for $\phi = 0$ we have a simple 1D tight binding model with alternating sites, A and b, and we have disconnected c sites, leading to localized states; for $\phi = \pi$ we have three connected sites that repeat N_c times, leading to localized states and to three energy levels N_c times degenerate.

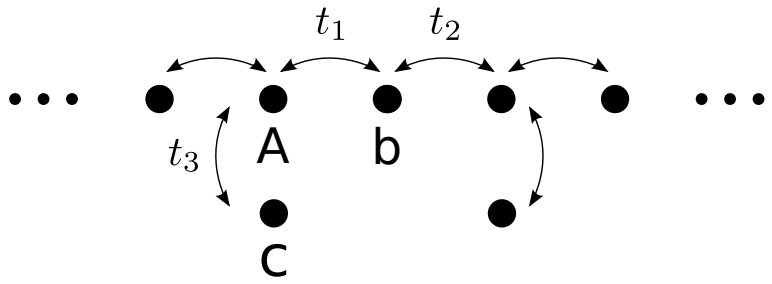

Figure 2.9: The Hamiltonian of the diamond chain threaded by an arbitrary flux can be mapped into a periodic Anderson like model (non interacting) with a basis of three sites per flux, the hopping amplitudes being controlled by the flux. In the particular case of zero flux we obtain a N_c cells Ab chain with hopping amplitude $\sqrt{2}t$ and N_c isolated sites that give rise to localized eigenstates. For the case of half flux quantum we obtain a system consisting in N_c times a three sites tight binding model with open boundary conditions and hopping amplitude $\sqrt{2}t$.

Let us transform the Hamiltonian into momentum space by performing the inverse Fourier transforms of the creation operators,

$$\begin{Bmatrix} A_j^\dagger \\ b_j^\dagger \\ c_j^\dagger \end{Bmatrix} = \frac{1}{\sqrt{N_c}} \sum_j \mathrm{e}^{-\mathrm{i}kj} \begin{Bmatrix} A_k^\dagger \\ b_k^\dagger \\ c_k^\dagger \end{Bmatrix}, \tag{2.26}$$

Substituting in the Hamiltonian and using the orthogonality condition, Eq. 1.31, we have,

$$H = -\sqrt{2}t \sum_k \left(1 + \cos(\phi/2)\mathrm{e}^{-\mathrm{i}k}\right) A_k^\dagger b_k + \sin(\phi/2)\mathrm{e}^{-\mathrm{i}k} A_k^\dagger c_k + \mathrm{h.c.} \tag{2.27}$$

The Hamiltonian is now block diagonal in the basis $\left\{A_k^\dagger, b_k^\dagger, c_k^\dagger\right\}|0\rangle$, having the form $H = \oplus_k H_k$ where H_k is,

$$H_k = -\sqrt{2}t \begin{pmatrix} 0 & 1 + \cos(\phi/2)\mathrm{e}^{-\mathrm{i}k} & \sin(\phi/2)\mathrm{e}^{-\mathrm{i}k} \\ 1 + \cos(\phi/2)\mathrm{e}^{\mathrm{i}k} & 0 & 0 \\ \sin(\phi/2)\mathrm{e}^{\mathrm{i}k} & 0 & 0 \end{pmatrix}. \tag{2.28}$$

By diagonalizing H_k we trivially diagonalize the full Hamiltonian H. Its eigenvalues are,

$$\begin{aligned} \epsilon_d &= 0, \\ \epsilon_\pm &= \pm 2t\sqrt{1 + \cos(\phi/2)\cos(k)}, \end{aligned} \tag{2.29}$$

and the associated operators that create the eigenvectors are,

$$\begin{aligned}\epsilon_+ &\rightarrow f_k^\dagger \left(A_k^\dagger, b_k^\dagger, c_k^\dagger\right), \\ \epsilon_d &\rightarrow a_k^\dagger \left(A_k^\dagger, b_k^\dagger, c_k^\dagger\right), \\ \epsilon_- &\rightarrow d_k^\dagger \left(A_k^\dagger, b_k^\dagger, c_k^\dagger\right),\end{aligned} \tag{2.30}$$

where, as seen previously, $f_k^\dagger$ creates a particle with momentum k on the top band, $a_k^\dagger$ on the dispersionless, flat band, and $d_k^\dagger$ on the bottom band.

We are primarily interested on the dispersionless band. The expression for the creation operator is,

$$a_k^\dagger = \frac{1}{\sqrt{2}\sqrt{1+\cos(\phi/2)\cos(k)}}\left[-\mathrm{e}^{-\mathrm{i}k/2}\sin(\phi/2)b_k^\dagger + \left(\mathrm{e}^{\mathrm{i}k/2} + \mathrm{e}^{-\mathrm{i}k/2}\cos(\phi/2)c_k^\dagger\right)\right]. \tag{2.31}$$

Or in a form that is more convenient for some calculations,

$$a_k^\dagger = \frac{1}{\sqrt{1+\cos\left(\phi/2\right)\cos(k)}}\left[\cos\left(\phi/4 - k/2\right)B_k^\dagger - \cos\left(\phi/4 + k/2\right)C_k^\dagger\right]. \tag{2.32}$$

Let us now examine or results in more detail. It is easily seen that for $\phi = 0, \pi$ we recover the already seen solutions. As it stands, this operator is not easily transformed into the real space. We can however work in a non-orthogonal basis, where the Fourier transform is easily done.

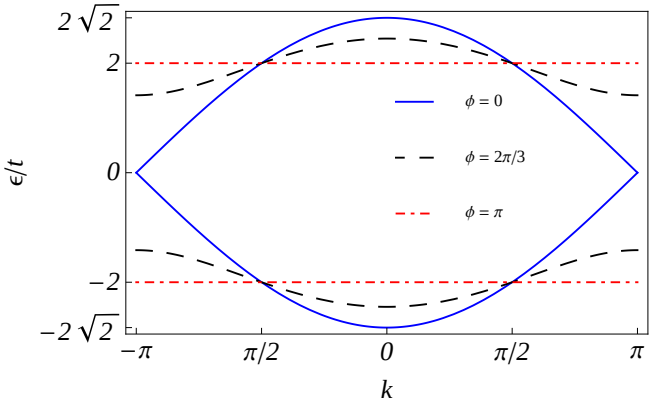

Figure 2.10: Dispersion relation of the diamond chain for different flux values (we have omitted the flat band $\epsilon_k = 0$ since it is not affected by the flux). Note that for $\phi = 0$ the system is gapless but a finite flux opens a gap between the bottom and the top band achieving its maximum value for $\phi = \pi$. On the other hand the badwidth decreases with finite flux, achieving its minimum value for $\phi = \pi$.

By doing so, we will not preserve the canonical anti-commutation relations, and we must be careful with inner products. Nevertheless it is worth it, since we are able to work in a localized eigenbasis, useful, for example when working, with perturbation theory in the case of a localized impurity.

For $\phi = 0$ the system is gapless. However, for finite ϕ a gap between the top and the bottom band develops. It is given by,

$$\Delta\epsilon = 4t\sqrt{1-\cos(\phi/2)}. \tag{2.33}$$

The bandwidth is also affect by the flux,

$$W = 4t\sqrt{1+\cos\left(\phi/2\right)}. \tag{2.34}$$

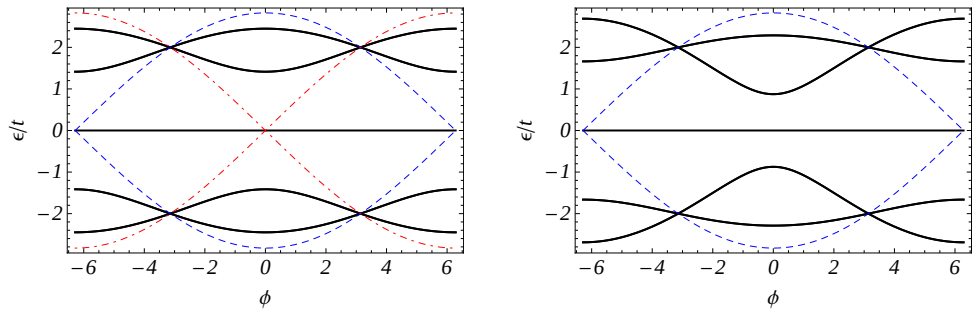

(a) Even N_c (b) Odd N_c

Figure 2.11: Single particle energy-flux plot for an even ($N_c = 6$) and an odd ($N_c = 7$) number of unit cells. The dispersive states for $k = 0$ correspond to the blue dashed curves and for $k = \pi$ to the red dot-dashed curves. Note that for even N_c for $\phi \notin [-\pi, \pi]$, the states interchange their energy value, when compared to the interval $\phi \in [-\pi, \pi]$ and therefore the properties of the system are 2π periodic on the flux. On the other hand for odd N_c there is an absence of a state with $k = \pi$ which makes the properties of the system 4π periodic on the flux

In fig 2.10 we show a plot of the dispersion relation of the diamond chain for several values of flux.

Let us for now address particularly the dispersive eigenvalues of the Hamiltonian. It is easily seen that when $k = \pi/2$, two flux independent eigenvalues appear. This condition is only fullfilled if the number of unit cells is a multiple of four, $N_c = 4n$ with n integer.

We can now fully appreciate the already studied particular situations $\phi = 0, \pi$. It is easily seen, that for $\phi = \pi$, the eigenvalues do not depend on the momentum, giving rise to a highly degenerate three level system. Note that for $\phi = \pi$ the system has always three levels, independently of the size of the chain, i.e., the number of unit cells. This three level behavior might be used, for example, to construct qutrits (quantum trits).

We should also note that it is now understandable why the system is 2π periodic on the flux when N_c is even and 4π periodic when N_c is odd. A flux of 2π interchanges the energies of the dispersive states with $k = 0$ and $k = \pi$. Since this two values of momentum are permitted when N_c is even, this brings nothing new. But because the value $k = \pi$ is forbidden when N_c is even, the period of the system is 4π on the flux (see Fig. 2.11). However, the dependence of the system on the parity reduces as the number of cells is increased and for a large number of cells, a 2π period, equivalent to the infinite case, can be assumed independently on the parity of the number of cells. In fact the minimum value of momentum in the FBZ when N_c is odd is,

$$k_{min} = -\pi \frac{N_c - 1}{N_c}, \tag{2.35}$$

and therefore when $N_c \gg 1$, it is justified to assume a period of 2π on the flux.

Chapter 3

Electronic and thermodynamic properties of the diamond chain

In this chapter we study the electronic and thermodynamic properties of the diamond chain threaded by an arbitrary flux. We will begin by calculating the density of states (DOS) of the diamond chain followed by the calculation of the persistent currents in the system. We then calculate the group velocity and effective mass of the electrons, important quantities for the transport properties of the system. We also study the the relation between the filling of the system and the Fermi energy and calculate the ground state energy. To conclude the chapter we address the thermodynamic properties of the diamond chain.

3.1 Density of states

Let us consider the thermodynamic limit (k continuous) and calculate the DOS of the dispersive branches (the DOS of the non dispersive branch is simply a Dirac delta). In 1D, the DOS is given by,

$$D(\epsilon) = \frac{1}{2\pi}\int_{-\pi}^{\pi} \delta(\epsilon - \epsilon_k(k))\mathrm{d}k. \tag{3.1}$$

Since $\epsilon_+(k) = -\epsilon_-(k)$ the DOS will be an even function of the energy. We also note that there is no crossing between the top and lower branches (bands) except when $\phi = 0$ and $\epsilon_+ = \epsilon_- = 0$. Let us then calculate the DOS for the ϵ_+ branch. One useful property of the Dirac delta function is that,

$$\delta(g(k)) = \sum_i \frac{\delta(k - k_i i)}{|g'(k_i)|}, \tag{3.2}$$

where k_i are the roots of $g(k)$. Therefore, defining $g(k) = \epsilon - \epsilon_k(k)$ we have,

$$D(\epsilon) = \frac{1}{2\pi}\sum_i \frac{1}{|g'(k_i)|}, \tag{3.3}$$

and thus the problem of finding the DOS has turned into a root finding problem. In our case we have,

$$g(k) = \epsilon - 2t\sqrt{1 + \cos(\phi/2)\cos(k)}. \tag{3.4}$$

The roots of $g(k)$ are given by,

$$k_\pm = \pm \arccos\left[\frac{\left(\frac{\epsilon}{2t}\right)^2 - 1}{\cos(\phi/2)}\right], \tag{3.5}$$

while the derivative of $g(k)$ is given by,

$$g'(k) = \frac{t\cos(\phi/2)\sin(k)}{\sqrt{1 + \cos(\phi/2)\cos(k)}}. \tag{3.6}$$

Calculating $g'(k_i)$ and substituting in Eq. (3.3) one obtains,

$$D_+(\epsilon_+) = \frac{1}{\pi t}\frac{\epsilon_+}{2t}\frac{1}{\sqrt{\cos^2(\phi/2) - \left((\epsilon_+/2t)^2 - 1\right)^2}}, \qquad \epsilon_+ \in \left[0, 2\sqrt{2}\right]. \tag{3.7}$$

Since the two branches only intersect at $\epsilon = 0$ (and their DOS is finite there), we can write for the combined DOS of the two branches,

$$D(\epsilon')_\pm = \frac{1}{\pi t}|\epsilon'|\frac{1}{\sqrt{\cos^2(\phi/2) - (\epsilon'^2 - 1)^2}}, \tag{3.8}$$

where,

$$\epsilon' = \frac{\epsilon}{2t}, \qquad \in \left[-\sqrt{2}, \sqrt{2}\right]. \tag{3.9}$$

The full DOS of the system considering that the dispersionless band is N_c times degenerate, and that we have been calculating the DOS per length/unit cell is therefore,

$$D(\epsilon) = D_\pm(\epsilon) + \delta(\epsilon). \tag{3.10}$$

A graphic of the DOS ($D_\pm(\epsilon)$) as a function of ϵ' for several values of flux is plotted in Fig. 3.1. It can be seen, as already discussed, that there is no gap for $\phi = 0$, but a finite flux opens one (it in fact lifts the degeneracy at the corner of the Brillouin zone). It can also be seen that when $\phi = \pi$ the DOS is zero everywhere and diverges for $\epsilon = 0, \pm 2t$. This a consequence of the fact that for that specific flux we have a three level system with energies $\epsilon = 0, \pm 2t$.

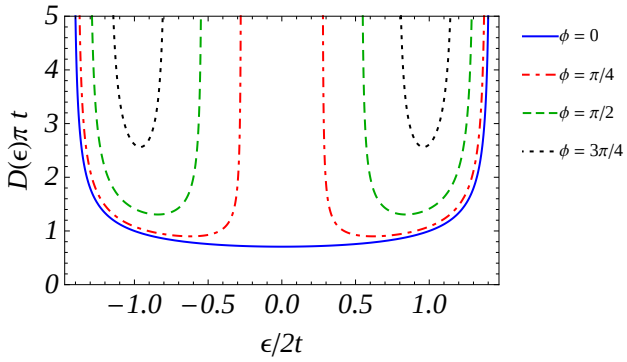

Figure 3.1: DOS of the diamond chain for several values of flux. Note the absence of a gap for $\phi = 0$

3.2 Persistent currents

It is known that quantum rings give rise to persistent currents when threaded by a magnetic flux. [16] These currents resemble superconducting currents altough the mechanism behind them is completely different; for quantum rings it is the AB effect that is responsible for persistent currents. Let us then calculate the persistent currents of the system. The one particle persistent current is given by, [17]

$$I_k = -\frac{2\pi}{\phi_0}\frac{\partial \epsilon_k}{\partial \phi}, \tag{3.11}$$

The one particle current for the middle flat band is trivially zero while for the top and bottom bands is given by,

$$I_\pm = \pm\frac{\pi}{\phi_0}t\frac{\sin(\phi/2)\cos(k)}{\sqrt{1 + \cos(\phi/2)\cos(k)}}, \tag{3.12}$$

where the positive solution refers to the top band and the negative one to the bottom band. Obviously the current for the top band is symmetric to that of the bottom band. It can easily be seen, that for $k = \pi/2$, the current is zero, giving rise to the already mentioned flat flux dependence band. A plot of the current for the bottom band for several values of flux is given in Fig. 3.2.

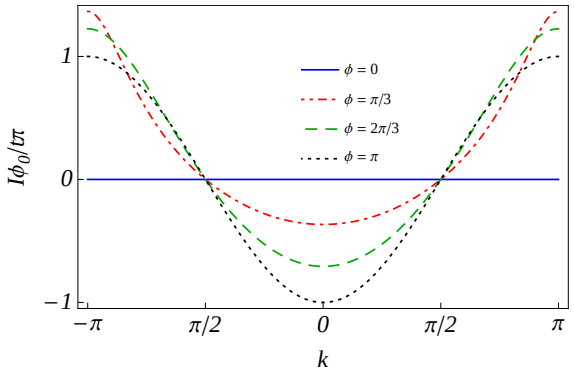

Figure 3.2: Single particle current for the bottom band ($\epsilon_-(k)$). Note that for $\phi = 0$ the persistent currents are inexistent and that states with $k = \pm\pi/2$ do not contribute to the total persistent current of the system independently of the flux.

3.3 Group velocity and effective mass

Some important quantities when treating effective free (quasi) particles are their group velocity and effective mass. These can, for example, be used to calculate semi-classical equations of motion in the presence of external fields. The velocity of an electron is given by its group velocity,

$$v_g = \frac{\partial \omega}{\partial k} = \frac{1}{\hbar}\frac{\partial \epsilon_k}{\partial k}, \tag{3.13}$$

while we can define an effective mass for the electron based on the second derivative of the single particle dispersion relation,

$$m^* = \frac{1}{\hbar}\left(\frac{\partial^2 \epsilon_k}{\partial k^2}\right)^{-1}. \tag{3.14}$$

In our tight binding case, this gives us for the dispersive bands,

$$\begin{aligned} v_g^{\pm} &= \mp\frac{1}{\hbar}\frac{t\cos(\phi/2)\sin(k)}{\sqrt{1+\cos(\phi/2)\cos(k)}}, \\ m_{\pm}^* &= \mp\frac{1}{\hbar^2}\frac{(1+\cos(\phi/2)\cos(k))^{3/2}}{t\cos^2(\phi/2)}, \end{aligned} \tag{3.15}$$

where v_g^+ and m_+^* refer to the top band and v_g^- and m_-^* refer to the bottom band. For the dispersionless band we have trivially,

$$\begin{aligned} v_g^d &= 0, \\ m_d^* &\to \infty. \end{aligned} \tag{3.16}$$

For $\phi = 0$, $k \to -\pi$ we have for the dispersive bands,

$$\begin{aligned} m_{\pm}^* &\to 0, \\ v_g^{\pm} &\to \mp\frac{\sqrt{2}t}{\hbar}, \end{aligned} \tag{3.17}$$

and therefore, the electrons behave as Dirac particles. Note that only for $\phi = 0$ is it possible to have a non zero velocity at the zone corner since the flux destroy the Dirac 1D-cones. For $\phi = \pi$ we have that in any band,

$$\begin{aligned} m^* &\to \infty, \\ v_g &= 0, \end{aligned} \tag{3.18}$$

and consequentially we have no transport when $\phi = \pi$.

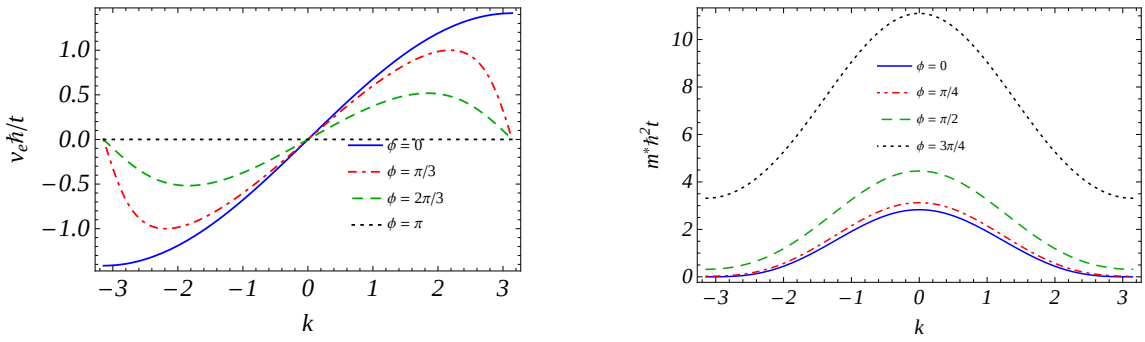

(a) Group velocity

(b) Effective mass

Figure 3.3: Electron group velocity and effective mass in the bottom band as a function of the momentum for several values of flux.

Eq. (3.16) implies that for zero temperature, transport is completely blocked at half-filling and our system behaves as an insulator. Finite ϕ opens a gap between the middle flat band and the top and bottom bands, which for $\phi = \pi$ is of order of the hopping amplitude, t. Since for normal materials t is of order 10^0, 10^{-1} eV, as an example for graphene $t \approx 2.8$ eV, [18] and since $1/k_B \approx 10^4$ k/eV, our system should behave as an insulator up to room temperature for $\phi \approx \pi$, while for smaller values of ϕ it will gradually become semiconducting. The magnetic flux allow us then to tune the properties of our system and at room temperature this insulator/semiconductor behavior dependent on the flux could be used to make logic gates.

3.4 Dependence of the filling on the Fermi energy

We define filling as the number of electrons, N_e, per number of sites, N_s,

$$\overline{n} = \frac{N_e}{N_s} = \frac{N_e}{3N_c}. \tag{3.19}$$

The number of states per unit cell in the energy interval $\epsilon \in [\epsilon_a, \epsilon_b]$ is given by,

$$n_s([\epsilon_a, \epsilon_b]) = \int_{\epsilon_a}^{\epsilon_b} D(\epsilon) \mathrm{d}\epsilon. \tag{3.20}$$

Since we are neglecting spin, each state can accommodate only one electron (if we want to include spin, the only difference is a factor of 2, $\overline{n} = 2n_s$). Due to the symmetrical nature of the energy spectrum and since each band can accommodate 1 electron per unit cell, we know that half filling occurs for $E_F = 0$. However, because the flat band contains N_c states we know that when $\overline{n} \in [1/3, 2/3]$ we have $E_F = 0$. Therefore, we only have to calculate the filling when E_F lies on the bottom or top bands. If E_F lies on the bottom band we have,

$$\overline{n} = \frac{1}{3} \int_{\epsilon_{b,\min}}^{E_F} D_-(\epsilon) \mathrm{d}\epsilon, \tag{3.21}$$

where $\epsilon_{b,\min} = -2\sqrt{2}t\cos(\phi/4)$ is the bottom of the band and where the factor of 1/3 is due to the fact that the integral of the DOS over a band is (each band contributes equally to the DOS),

$$\int_{\text{Band}} D(\epsilon)\mathrm{d}\epsilon = 1, \tag{3.22}$$

and we have three bands. Using Eq. (3.8) we have,

$$\overline{n} = \frac{1}{3}\frac{1}{2\pi}\left[\arctan\left(\frac{\epsilon'_{b,\min}}{\sqrt{\cos^2(\phi/2) - \epsilon'^2_{b,\min}}}\right) - \arctan\left(\frac{E'_F}{\sqrt{\cos^2(\phi/2) - E'^2_F}}\right)\right], \tag{3.23}$$

where,

$$\begin{aligned} \epsilon'_{b,\min} &= \left(\frac{\epsilon_{b,\min}}{2t}\right)^2 - 1, \\ E'_F &= \left(\frac{E_F}{2t}\right)^2 - 1. \end{aligned} \tag{3.24}$$

If, on the other hand, E_F lies on the top band, the situation is identical, except that we have to consider that two bands are already filled and that the expression for the band minimum is now different. We therefore have,

$$\overline{n} = \frac{2}{3} + \frac{1}{3}\int_{\epsilon_{t,\min}}^{E_F} D_+(\epsilon)\mathrm{d}\epsilon, \tag{3.25}$$

where $\epsilon_{t,\min} = 2\sqrt{2}t\sin(\phi/4)$ is the bottom of the top band. This will give us a relation identical to that above.

3.5 Ground state energy

Given the results of the preceding section, we are able to calculate the ground state energy of the system as a function of the filling. The ground state energy is given by,

$$E_{\text{g.s.}} = \int_{E_{\min}}^{E_F} D(\epsilon)\epsilon\mathrm{d}\epsilon, \tag{3.26}$$

while Eq. (3.23) and (3.24) give us the relation between the Fermi energy and the filling. For a general value of ϕ there is no simple analytical expression and the ground state energy should be calculated numerically. However, when $\phi = \pi$ it is very simple to derive an exact result. Given that the system only has three energy levels, $\epsilon = 0, \pm 2t$ and that each can take N_c electrons, the ground state energy per unit cell while the bottom band is not fully filled is given by $E_{\text{g.s.}} = -2tN_e/N_c = -6t\overline{n}$. At $\overline{n} = 1/3$ the bottom band gets fully filled and from $\overline{n} = 1/3$ to $\overline{n} = 2/3$ we are filling the middle band whose energy is $\epsilon = 0$. Therefore $E_{\text{g.s.}} = -2t, \quad \overline{n} \in [1/3, 2/3]$. For $\overline{n} > 2/3$ we start filling the upper band, whose energy is $\epsilon = 2t$. In this situation the ground state energy is given by, $E_{\text{g.s.}} = 6t(\overline{n} - 2/3) - 2t$. Combining these results, the ground state energy as a function of filling for $\phi = \pi$ is given by,

$$\frac{E_{\text{g.s.}}}{t} = \begin{cases} -6\overline{n} & ,\overline{n} \in [0, 1/3[\\ -2 & ,\overline{n} \in [1/3, 2/3] \\ 6(\overline{n} - 2/3) - 2 & ,\overline{n} \in]2/3, 1] \end{cases} \tag{3.27}$$

In Fig. 3.4 we plot the ground state energy as function of filling for several values of flux. As can be seen for $\overline{n} \in [1/3, 2/3]$ the ground state energy remains constant since we are filling the flat band $\epsilon_k = 0$. The ground state energy is obviously even around $\epsilon_k = 0.5$ due to the symmetric nature of the dispersion relation. We also see that for $\overline{n} \notin [1/3, 2/3]$ the dependence of the ground state energy on the filling departs from its linear behavior when $\phi \neq \pi$.

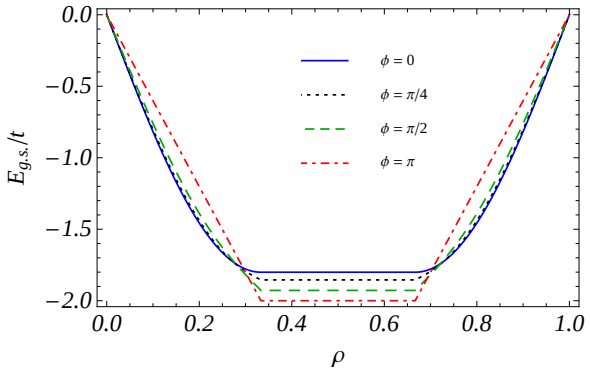

Figure 3.4: Ground state energy in the thermodynamic limit as a function of filling for several values of flux. Note that $E_{\text{g.s.}}$ remains constant when we are filling the flat band, $\overline{n} \in [1/3, 2/3]$ achieving its minimum value on that interval for $\phi = \pi$. Note also that for $\phi \neq \pi$ $E_{\text{g.s.}}$ departs from its linear behavior on $\overline{n}$.

3.6 Thermodynamics

The Hamiltonian of our system,

$$H = \sum_k \epsilon_+(k,\phi)\left(f_k^\dagger f_k - d_k^\dagger d_k\right), \tag{3.28}$$

with,

$$\epsilon_+(k,\phi) = 2t\sqrt{1+\cos(\phi/2)\cos(k)}, \tag{3.29}$$

is that of a three level multimode fermionic oscillator (see appendix A for a thermodynamic description of a single level, single mode fermionic oscillator). Therefore, considering a grand canonical description, and neglecting spin (the physics is basically the same since we are considering non-interacting electrons), we will have, 8 states per mode.[1] Since the modes are independent, the grand canonical partition function of the system is given by the product of the partition function of each mode,

$$Z = \prod_k Z_k, \tag{3.30}$$

where Z_k is the partition function of a mode with momentum k,

$$Z_k = \mathrm{e}^{3\beta\mu} + \mathrm{e}^{\beta(\epsilon_+ + 2\mu)} + \mathrm{e}^{2\beta\mu} + \mathrm{e}^{\beta(-\epsilon_+ + 2\mu)} + \mathrm{e}^{\beta(\epsilon_+ + \mu)} + \mathrm{e}^{\beta\mu} + \mathrm{e}^{\beta(-\epsilon_+ + \mu)} + 1. \tag{3.31}$$

In this situation the thermodynamic properties of the system we will be interested in will be given by a sum of the thermodynamic properties of the several modes,

$$\begin{Bmatrix} \overline{n} \\ \overline{E} \\ c_v \end{Bmatrix} = \sum_k \begin{Bmatrix} \overline{n}_k \\ \overline{E}_k \\ c_v^k \end{Bmatrix}. \tag{3.32}$$

We will start by studying the single mode thermodynamics properties. The average occupation number is given by,

$$\overline{n}_k = \sum_{j=\text{states}} n_j \mathrm{e}^{-\beta(\epsilon_j - n_j\mu)} = \frac{\partial \ln Z_k}{\partial \mu}, \tag{3.33}$$

and it can be seen that while a general value of filling depends on β, ϵ_+ and μ, half filling always occurs for $\mu = 0$ independently of ϵ_+ or the temperature. This is a consequence of the fact that

[1] This is simply the sum of the elements of the third row of Pascal's triangle, 2^3.

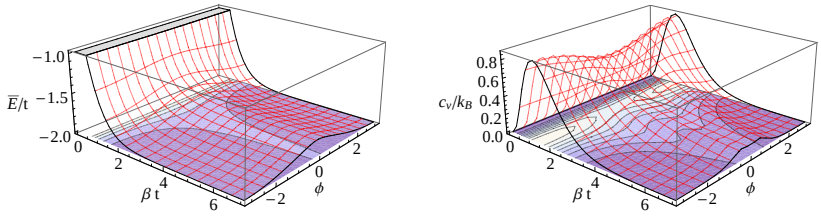

(a) Mean energy (b) Specific Heat

Figure 3.5: Mean energy and specific heat for an infinite system.

our system is a three level system symmetric around $\epsilon = 0$. At half filling we can get simple expressions for the mean energy and for the specific heat. The mean energy for a single mode, at half filling, is given by,

$$\overline{E}_k = -\epsilon_+ \frac{\sinh(\beta\epsilon_+)}{1+\cosh(\beta\epsilon_+)}, \tag{3.34}$$

while the specific heat is given by,

$$c_v^k = k_B(\epsilon_+\beta)^2 \frac{\cosh(\beta\epsilon_+)}{(1+\cosh(\beta\epsilon_+))^2}. \tag{3.35}$$

Note that these are quite general expressions valid for any three level system system with $\epsilon = 0, \pm\epsilon_+$.

In the continuum limit, the thermodynamic variables per unit cell can be calculated by replacing the sum in eq. (3.32) by an integral according to (in our one dimensional case),

$$\sum_k \to \frac{1}{2\pi}\int_{-\pi}^{\pi} \mathrm{d}k. \tag{3.36}$$

At half-filling it is possible to find closed form asymptotic expressions at high and low temperature for the mean energy and specific heat in the thermodynamic limit. To do so we use the asymptotic expressions for the single mode mean energy and specific heat: At high temperature, $\beta\epsilon_+ \ll 1$,

$$\begin{aligned} \overline{E}_k &\approx \frac{\epsilon_+^2\beta}{2} \\ c_v &\approx \frac{k_B(\epsilon_+\beta)^2)}{4} \end{aligned} \tag{3.37}$$

And at low temperature, $\beta\epsilon_+ \ll 1$,

$$\begin{aligned} \overline{E}_k &\approx -\epsilon_+ \\ c_v &\approx 0 \end{aligned} \tag{3.38}$$

Integrating these expressions one obtains the asymptotic behavior of energy in the thermodynamic limit,

$$\overline{E} \approx \begin{cases} -2t^2\beta, & \beta\epsilon_+ \ll 1 \\ -4t\sqrt{1-\cos(\phi/2)}\,\mathrm{E}_2\left(1-\cot^2(\phi/4)\right), & \beta\epsilon_+ \gg 1 \end{cases} \tag{3.39}$$

where, $\mathrm{E}_2(k)$ is the complete elliptic integral of the second kind[2] We also obtain, for the specific heat in the thermodynamic limit,

$$c_v \approx \begin{cases} k_B\beta^2t^2, & \beta\epsilon_+ \ll 1 \\ 0, & \beta\epsilon_+ \gg 1 \end{cases} \tag{3.40}$$

The plots of the mean energy and specific heat at half filling for finite temperature, obtained by numerical integration are shown in Fig. 3.5.

[2]This is not, however, a truly closed form expression, but since it is a well known function, we decided to include it in the definition.

Chapter 4

Diamond star and connecting the diamond

Periodic boundary conditions are often used simply as a mathematical convenience for very large open systems. We have already discussed that our system can have a period of 2π or 4π on the flux depending on the parity of N_c. In this chapter we study in more detail the effect of the periodic boundary conditions for a finite system and we also introduce an extra magnetic flux in the interior of the chain. We also address the problem of allowing hops between next nearest neighbors which destroy, as we shall see, the flatness of the middle band.

4.1 Diamond star

Up until now we have been treating our system using periodic boundary conditions but we have not discussed if we were using them as a mere mathematical convenience for a large linear system or if we were in fact treating a periodic finite size system. While for an infinite system, the parity of the number of rings is unimportant, we have seen that due to finite size effects the properties of a truly finite periodic system have a different periodicity depending on whether the number of cells is even or odd. Here we address the problem of a truly periodic system with a magnetic flux ϕ threading the smaller diamond rings and a magnetic flux ϕ_o threading the major ring, as depicted in Fig. 4.1. We shall call this system a *diamond star* and reserve this name for small sized periodic systems such as molecules. Note that there are two ways to close the ring, either by leaving the B sites on the interior of the ring or the C sites. The two situations are identical apart from a different sign on the flux and therefore we will assume that we have closed our ring so as to leave the C sites on the interior. This system can be used to model molecular systems with such topology, which might be useful for the field of molecular electronics. One well known example of similar topology are cyclic aromatic compounds where instead of four sites rings we have benzene's six sites rings.

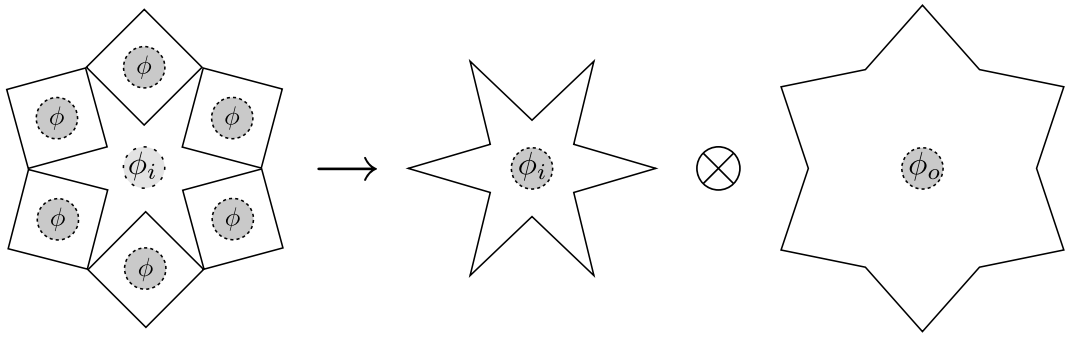

Figure 4.1: A diamond star: a system of periodic diamond rings. In this case we consider that each diamond ring is threaded by a flux ϕ while the inner star itself is threaded by a flux ϕ_i. This system can be factorized into an outer ring with flux ϕ_o and an inner ring with a flux ϕ_i - we must however be careful to remember that these two rings share the A sites.

We can factorize our system into two rings, an outer one and an inner one, while keeping in mind

that they share the A sites and that they are, therefore, coupled. This is depicted schematically in Fig. 4.1. An electron travelling through the outer ring sees and effective flux ϕ_o while and electron travelling through the inner ring sees a different effective flux ϕ_i,

$$\begin{aligned}\phi_o &= \phi' + 2N_c\frac{\phi}{4},\\ \phi_i &= \phi' - 2N_c\frac{\phi}{4}.\end{aligned} \tag{4.1}$$

We also note that in the limit of vanishing ϕ', this effective flux still remains non zero. The Hamiltonian of our system is given by,

$$\begin{aligned}H = &- t\sum_{j=1}^{N_c} \mathrm{e}^{\mathrm{i}\phi_o/2N_c}A_j^\dagger B_j + \mathrm{e}^{\mathrm{i}\phi_i/2N_c}C_j^\dagger A_j + \\ &\mathrm{e}^{\mathrm{i}\phi_i/2N_c}A_{j+1}^\dagger C_j + \mathrm{e}^{\mathrm{i}\phi_o/2N_c}B_j^\dagger A_{j+1} + \mathrm{h.c.}.\end{aligned} \tag{4.2}$$

By transforming into Fourier space the Hamiltonian is easily diagonalizable and we obtain for its spectrum,

$$\epsilon_k = 0, \pm 2t\sqrt{1+\cos(\phi/2)\cos(\phi'/N_c+k)}. \tag{4.3}$$

As we can see the insertion of a flux inside of the chain only translates the energy dispersion relation by ϕ'/N_c and therefore does nothing to the flat band. This result is expected since it is similar to what is observed in 1D quantum rings (section 1.3). We can therefore use ϕ' to control the momentum for which the top/bottom bands reach its maximum/minimum energy.

4.2 Connecting the diamond

We will now address the problem of introducing hops between second neighbors. We will consider two different situations, one in which we introduce hops inside the diamond and one in which we introduce hopings between next nearest neighbors B sites and next nearest neighbors C sites.

4.2.1 Internal hops

We will now address the problem of introducing hops inside the diamond, as depicted in Fig. 4.2. We will consider that hops between B and C sites are equal to those between adjacent A sites, i.e., a perfect diamond. One could easily make these hops different and distort the diamond, however the physics would be similar and we restrict ourselves to the simplest problem. Note that we will not introduce any Zeeman term since it does not have a great impact in our solution. Its main effect is to lift some degeneracies if we consider this to be a spinful system. The Hamiltonian with the additional hoppings is given by,

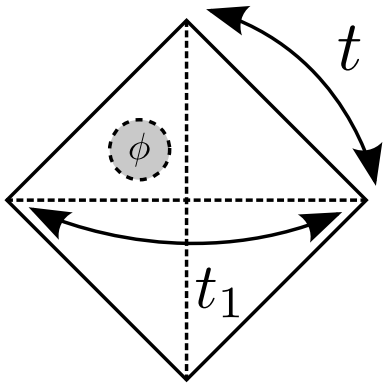

Figure 4.2: We consider that the electron can hop between adjacent A sites and between B and C sites on the same cell.

$$H = H_0 - t_1 \sum A_{j+1}^\dagger A_j + B_j^\dagger C_j + \text{h.c.}, \tag{4.4}$$

where H_0 is the Hamiltonian of Eq. (2.21). This Hamiltonian can be easily diagonalized in momentum space, becoming a block diagonal matrix in the single particle basis, $\left\{A_k^\dagger, B_k^\dagger, C_k^\dagger\right\}_k |0\rangle$. Such blocks are given by,

$$H_k = \begin{pmatrix} -2t_1\cos(k) & -2te^{-ik/2}\cos(\phi/4+k/2) & -2te^{-ik/2}\cos(\phi/4-k/2) \\ -2te^{ik/2}\cos(\phi/4+k/2) & 0 & -t_1 \\ -2te^{ik/2}\cos(\phi/4-k/2) & -t_1 & 0 \end{pmatrix}. \tag{4.5}$$

The secular equation does not have a simple solution for general flux. However for $\phi = 0$ the eigenvalues are given by,

$$\epsilon_k = \begin{cases} t1 \\ \frac{1}{2}\left(-t_1 - 2t_1\cos(k) \pm \sqrt{32t^2\cos^2(k/2) + t_1^2 - 4t_1^2\cos(k) + 4t_1^2\cos^2(k)}\right) \end{cases} \tag{4.6}$$

The flat band eigenstates of H_0, $a_k^\dagger |0\rangle$, are also eigenkets of the full Hamiltonian H,

$$H a_k^\dagger |0\rangle = t_1 a_k^\dagger |0\rangle . \tag{4.7}$$

Therefore, hops inside the diamond do not lift the degeneracy of the flat for $\phi = 0$ band but open a gap in the system.

Considering $t_1 \ll t$ and using first order perturbation theory for degenerate levels, we can find a correction to the flat band energies for $\phi \neq 0$, where the states $a_k^\dagger |0\rangle$ are not eigenstates of the full Hamiltonian. The corrected energies are found to be,

$$\epsilon_a(k) = -t_1 \frac{\cos(\phi/2) + \cos(k)}{1 + \cos(\phi/2)\cos(k)}, \tag{4.8}$$

and therefore for $\phi \neq 0$ the degeneracy of the flat bands is partially lifted, the maximum degeneracy now being 2.

In Fig. 4.3 one can see the effect of turning on the hopping inside the diamond while in Fig. 4.4 we compare the dispersion relations for several values of flux. As can be seen, the three bands for $\phi = \pi$ are no longer flat for finite t_1.

4.2.2 Internal and external hops

Here we consider the effect of not only adding hops inside of the diamond, like in the previous subsection, but also of adding hops between diamonds. We consider the possibility of having hops between B sites on adjacent cells and C sites on adjacent cells. We also assume, for simplicity, that the new hopping amplitude is equal to that describing the hops inside of the diamond. The Hamiltonian of our system is then,

$$H = H_{\text{in}} - t_1 \sum_j B_j^\dagger B_{j+1} + C_j^\dagger C_{j+1} + \text{h.c.}, \tag{4.9}$$

where H_{in} is the Hamiltonian of Eq. (4.4). Like before there is no general simple solution for the eigenvalues but considering $t_1 \ll t$ and using perturbation theory for degenerate levels we can find simple expressions for the energy of the middle band. Doing so we find,[1]

$$\epsilon_a = \frac{-t_1}{1 + \cos(\phi/2)\cos(k)} \left[\cos(k) + 2\cos^2(k)\cos(\phi/2 - \cos(\phi/2))\right]. \tag{4.10}$$

[1] Where we have considered the degenerate subspace $\epsilon = 0$ to be spanned by $\left\{a_k^\dagger\right\}_k |0\rangle$. Note however that for $\phi = 0$ and even N_c the top and bottom bands each contribute with one state to this degenerate subspace, as will be discussed in the next chapter.

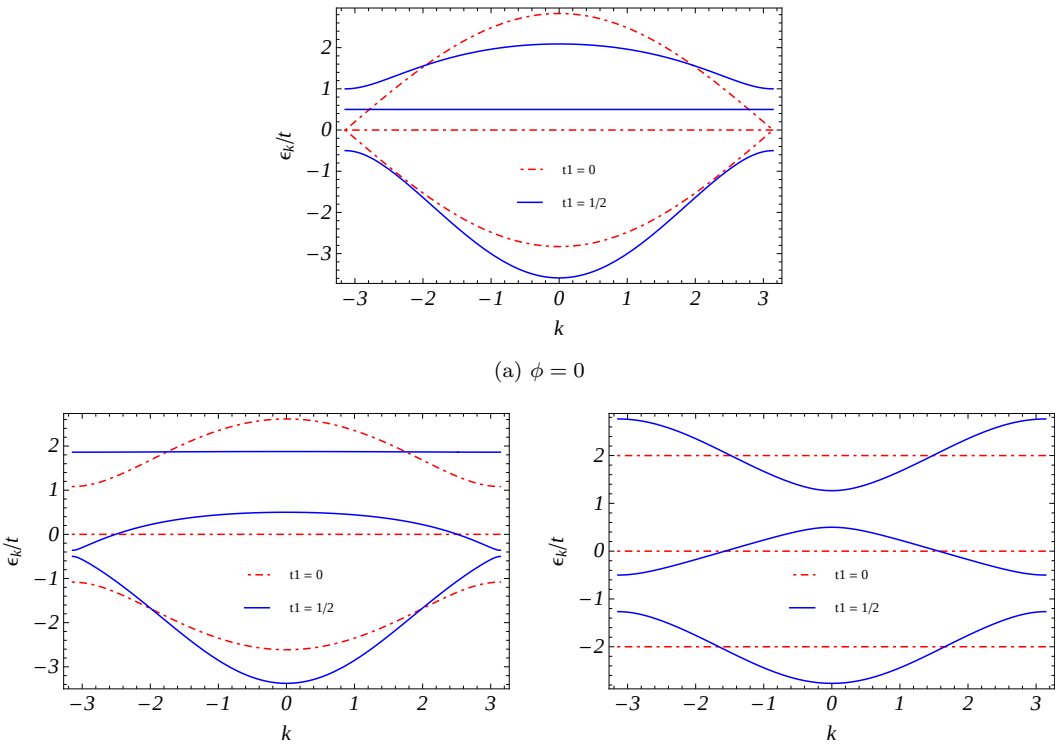

(a) $\phi = 0$

(b) $\phi = \pi/2$

(c) $\phi = \pi$

Figure 4.3: Comparison of the dispersion relations when the hoping inside of the diamond is turned on and off for several values of flux. Note that while for zero flux the effect on the flat band of turning on the hoping inside of the diamond is only to shift it, for finite flux it becomes dispersive.

The dispersion relations for several situations is plotted in Fig. 4.6 and 4.7 and as can be seen, the external hops turn the flat band dispersive even for $\phi = 0$, unlike in previous section. The external hops are also able of inverting the concavity of the bands, therefore changing the sign of the electron effective mass. As an example note that for $\phi = \pi$ considering only internal hops and $t_1 = 1/2$ we have that the effective mass around $k = 0$ is positive for the upper and lower bands but negative for the middle band as depicted in Fig. 4.3c. On the other hand, by turning on external hops we have that the effective mass around $k = 0$ is positive even for the middle band as depicted in Fig. 4.6c.

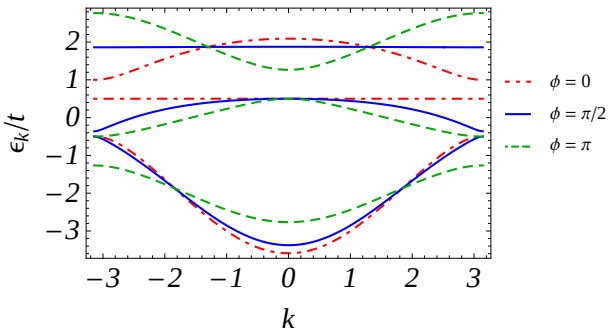

Figure 4.4: Dispersion relation by setting $t_1 = t/2$ for several values of flux. Note that there are still states whose energy is flux independent but unlike the situation $t_1 = 0$ these no longer have a momentum $k = \pm\pi/2$. Note also that for $k = 0$ the middle band has a flux independent energy equal to t_1.

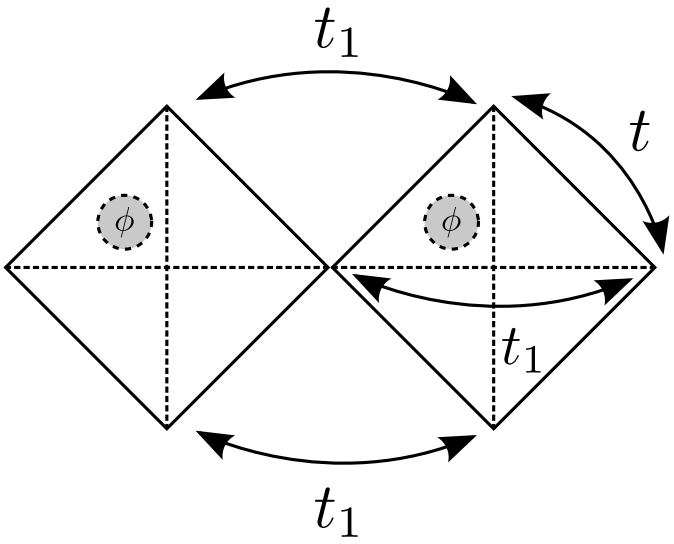

Figure 4.5: We consider the possibility of hops between nearest neighbors B sites and between nearest neighbors C sites.

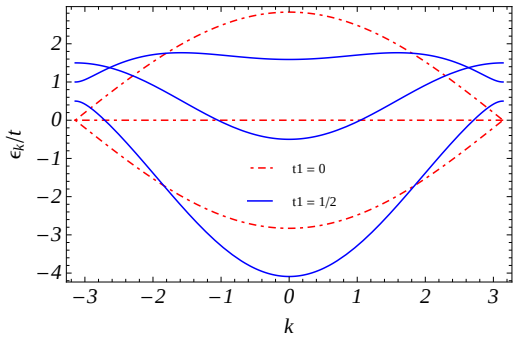

(a) $\phi = 0$

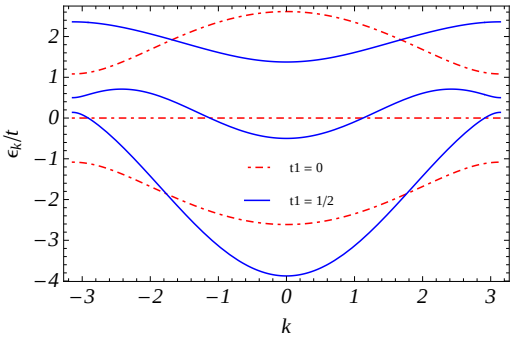

(b) $\phi = \pi/2$

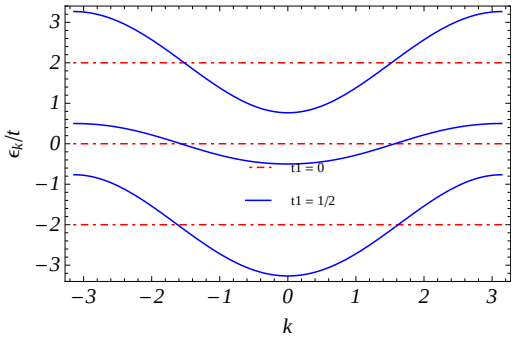

(c) $\phi = \pi$

Figure 4.6: Comparison of the dispersion relation when the hoping between the considered second nearest neighbors is turned on and off. Note that unlike in previous section, where we only considered hops inside of the diamond, by considering hops between next nearest neighbors B sites and next nearest neighbors C sites, the middle band becomes dispersive even for $\phi = 0$.

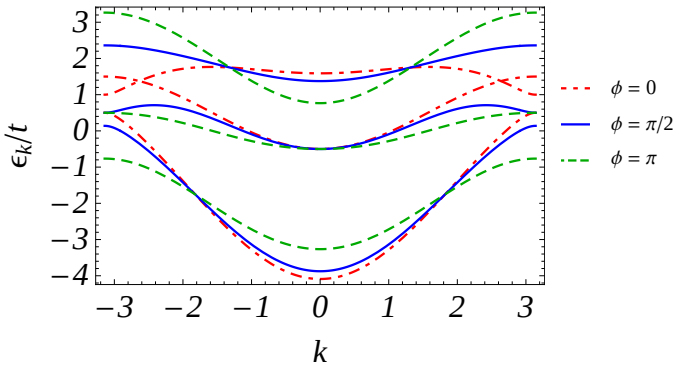

Figure 4.7: Dispersion relation by setting $t_1 = t/2$ for several values of flux. Note that there are still states whose energy is flux independent but like in previous section for $t_1 = 0$ these no longer have a momentum $k = \pm\pi/2$. Note also that for $k = 0$ the middle band has a flux independent energy equal to $-t_1$ (and not t_1 like in previous section).

Chapter 5

Impurities and ABC diamonds

In this chapter we consider the effect of adding disorder to our system. We will start by considering the effect of adding a single impurity to our system. We will consider either that this impurity has a different on-site energy from the rest of the system or that it has a different hopping amplitude to and from its nearest neighbors. Since this impurity breaks translational invariance we expect that it will lift at least some of the degeneracies present in our system. To conclude we will preserve translational invariance in our system but assume not only different on-site energies on the unit cell but also that the hopping amplitude between A and B sites is different to that between A and C sites.

5.1 Single localized impurity

Let us examine the degeneracies of the single particle eigenvalues for $\phi = 0$ for a spinless system. The top and lower band states with $k = 0$ are always non degenerate. When the number of unit cells N_c is odd, the states of these bands with momentum $k \neq 0$ are two times degenerate since the energy is even in k while the flat band states are N_c times degenerate. For N_c even, the situation is identical except that the top and lower band states with $k = -\pi$ have the same energy as the flat band states and together form a $N_c + 2$ times degenerate subspace. For $\phi = \pi$ the situation is simpler; the top band states are all degenerate (N_c times) and the same goes for the flat and lower band ones. We therefore have the following degenerate subspaces for $\phi = 0$ when N_c is odd,

$$\begin{aligned}
&\text{Subspace 1} : \left\{a_j^\dagger\right\}_j |0\rangle && \rightarrow \epsilon = 0 \\
&\text{Subspace 2} : \left\{d_{-k}^\dagger, d_k^\dagger\right\} |0\rangle && \rightarrow \epsilon = -2\sqrt{2}t\cos(k/2), \quad k \neq 0 \\
&\text{Subspace 3} : \left\{f_{-k}^\dagger, f_k^\dagger\right\} |0\rangle && \rightarrow \epsilon = +2\sqrt{2}t\cos(k/2), \quad k \neq 0
\end{aligned} \tag{5.1}$$

and when N_c is even,

$$\begin{aligned}
&\text{Subspace 4} : \left\{d_{-\pi}^\dagger, f_{-\pi}^\dagger, a_j^\dagger\right\}_j |0\rangle && \rightarrow \epsilon = 0 \\
&\text{Subspace 1a} : \left\{d_{-k}^\dagger, d_k^\dagger\right\} |0\rangle && \rightarrow \epsilon = -2\sqrt{2}t\cos(k/2), \quad k \neq -\pi, 0 \\
&\text{Subspace 2a} : \left\{f_{-k}^\dagger, f_k^\dagger\right\} |0\rangle && \rightarrow \epsilon = +2\sqrt{2}t\cos(k/2), \quad k \neq -\pi, 0
\end{aligned} \tag{5.2}$$

For $\phi = \pi$ the degenerate subspaces are simply,

$$\begin{aligned}
&\text{Subspace 7} : \left\{a_j^\dagger\right\}_j |0\rangle \rightarrow \epsilon = 0 \\
&\text{Subspace 8} : \left\{d_j^\dagger\right\}_j |0\rangle \rightarrow \epsilon = -2t \\
&\text{Subspace 9} : \left\{f_j^\dagger\right\}_j |0\rangle \rightarrow \epsilon = 2t
\end{aligned} \tag{5.3}$$

Since the degenerate states are in principle more affected by a small perturbation than the non degenerate ones, the effect of a single impurity on the system is studied using first order

perturbation theory for degenerate levels. Let us consider that our Hamiltonian is given by,

$$H = H_0 + U, \tag{5.4}$$

where H_0 is the unperturbed Hamiltonian given in Eq. (2.21) and U is a small perturbation. Let us first note that independently of U, the expression for the perturbed eigenstates and eigenenergies will always be the same for subspaces 1 and 1a and for subspaces 2 and 2a (to first order in U). Therefore we shall only concern ourselves with 7 degenerate subspaces. We will start by considering a single impurity in an A site with a different on-site energy, $\epsilon_A \ll 1$,

$$U = \epsilon_A A_n^\dagger A_n, \tag{5.5}$$

where n is an arbitrary site. In this situation, since the impurity is localized on an A site, it does not affect the eigenstates $a_k^\dagger |0\rangle$ and these remain eigenstates of the full Hamiltonian independently of the value of the flux. Therefore subspaces 1 and 7 are not affected by the perturbation (in any order). Note also that since for $\phi = \pi$ the eigenstates $d_j^\dagger |0\rangle$ and $f_j^\dagger |0\rangle$ are extremely localized, the impurity will, in this situation, only affect a single d state and a single f state namely those localized around the impurity, $d_n^\dagger |0\rangle$ and $f_n^\dagger |0\rangle$. This means that we can easily find an exact solution for the full Hamiltonian when $\phi = \pi$ using,

$$A_n^\dagger = \frac{1}{\sqrt{2}} \left(d_n^\dagger - f_n^\dagger \right). \tag{5.6}$$

The eigenvectors and eigenvalues of the full Hamiltonian remain those of H_0 except in the subspace of the impurity localized states, the two new eigenvalues and eigenvectors being,

$$\begin{aligned} c_+^\dagger &= \frac{1}{\sqrt{1+\epsilon_A'^2}} \left(f_n^\dagger + \epsilon_A' d_n^\dagger \right) \rightarrow \epsilon_+ = +2t\sqrt{1+\left(\frac{\epsilon_A}{2t}\right)}, \\ c_-^\dagger &= \frac{1}{\sqrt{1+\epsilon_A'^2}} \left(d_n^\dagger - \epsilon_A' f_n^\dagger \right) \rightarrow \epsilon_- = -2t\sqrt{1+\left(\frac{\epsilon_A}{2t}\right)}, \end{aligned} \tag{5.7}$$

where we have defined,

$$\epsilon_A' = \frac{\epsilon_A}{2t} \frac{1}{1+\sqrt{1+\left(\frac{\epsilon_A}{2t}\right)^2}}. \tag{5.8}$$

As expected these eigenvalues and eigenvectors reduce to the old ones (Eq. (2.19) and (2.20)) in the limit $\epsilon_A \rightarrow 0$. For $\phi = 0$ we calculated the perturbed eigensystem using first order perturbation theory assuming $\epsilon_A \ll 1$. The results are displayed in table 5.1. As could be expected, the effect of the impurity on the delocalized states decreases with increasing number of sites.

Let us now assume that the impurity in the A site has a different hoping amplitude to and from, the perturbation Hamiltonian being given by,

$$U = -\Delta t \left(\mathrm{e}^{\mathrm{i}\phi/4} C_n^\dagger A_n + \mathrm{e}^{\mathrm{i}\phi/4} A_n^\dagger B_n + \mathrm{e}^{\mathrm{i}\phi/4} A_n^\dagger C_{n-1} + \mathrm{e}^{\mathrm{i}\phi/4} B_{n-1}^\dagger A_n + \mathrm{h.c.} \right). \tag{5.9}$$

For $\phi = \pi$ it is easy to verify that the full Hamiltonian is diagonal in the eigenbasis of H_0,

$$H = -2t \sum_j \left(d_j^\dagger d_j - f_j^\dagger f_j \right) - 2\Delta t_A \left(d_n^\dagger d_n - f_n^\dagger f_n \right), \tag{5.10}$$

and therefore the eigenenergies remain the same except for those of the d and f states localized around the impurity whose energy now is $\epsilon = \pm 2t_A$, $t_A = t + \Delta t_A$ where the minus sign correspond to the d states. For $\phi = 0$ we considered a small perturbation, $\Delta t_A \ll 1$ and calculated the eigensystem using perturbation theory the results being displayed in table 5.2.

Let us now consider that our impurity resides on a B site (for a C site is identical since they are related by a symmetry operation). Like before let us first assume that it has a different on site energy from that of the other sites of the system. The perturbation Hamiltonian is,

$$U = \epsilon_B B_n^\dagger B_n. \tag{5.11}$$

For $\phi = \pi$ we now that the perturbation can only connect the six states localized around the impurity, namely, $\left\{d_{n,n+1}^\dagger, a_{n,n+1}^\dagger, f_{n,n+1}^\dagger\right\}|0\rangle$. Therefore the full Hamiltonian is diagonal in the eigenbasis of H_0 except for a 6×6 block which we must diagonalize. Doing so yields three simple eigenvalues and associated eigenvectors,

$$\begin{aligned}
&\frac{1}{\sqrt{2}}\left(\mathrm{i}a_n^\dagger + a_{n+1}^\dagger\right) \to \epsilon = 0,\\
&\frac{1}{\sqrt{2}}\left(\mathrm{i}d_n^\dagger - d_{n+1}^\dagger\right) \to \epsilon = -2t,\\
&\frac{1}{\sqrt{2}}\left(\mathrm{i}f_n^\dagger - f_{n+1}^\dagger\right) \to \epsilon = +2t,
\end{aligned} \tag{5.12}$$

the remaining three eigenvalues being given by the secular equation,

$$\epsilon^3 - \epsilon_B\epsilon^2 - 4t^2\epsilon + 2t^2\epsilon_B = 0 \tag{5.13}$$

and consequently there is no simple exact expression for the associated eigenvectors. The results for $\phi = 0$, calculated using first order perturbation theory, are displayed in table 5.3.

Let us now consider that the impurity in B site has a different hopping amplitude to and fro such that the Hamiltonian is given by,

$$U = -\Delta t_B B_n^\dagger\left(\mathrm{e}^{-\mathrm{i}\phi/4}A_n + \mathrm{e}^{\mathrm{i}\phi/4}A_{n+1}\right). \tag{5.14}$$

For $\phi = \pi$ this situation is identical to the previous one and the full Hamiltonian is diagonal in the eigenbasis of H_0 except for a 6×6 block which upon diagonalization give us the eigenvalues,

$$\epsilon = \begin{cases} 0 \quad (\times 2)\\ -2t\\ +2t\\ -\sqrt{2}\sqrt{2t^2 + 2t\Delta t_B + \Delta t_B^2}\\ +\sqrt{2}\sqrt{2t^2 + 2t\Delta t_B + \Delta t_B^2}\end{cases} \tag{5.15}$$

with the associated eigenvectors given, respectively, by

$$\begin{cases}
\frac{1}{\sqrt{2}}\left(\mathrm{i}a_n^\dagger + a_{n+1}^\dagger\right)\\
\frac{1}{2\sqrt{1+t'^2}}\left(\mathrm{i}d_n^\dagger + d_{n+1}^\dagger + \sqrt{2}t'(\mathrm{i}a_n^\dagger - a_{n+1}^\dagger) + \mathrm{i}f_n^\dagger + f_{n+1}^\dagger\right)\\
\frac{1}{\sqrt{2}}\left(\mathrm{i}d_n^\dagger - d_{n+1}^\dagger\right)\\
\frac{1}{\sqrt{2}}\left(\mathrm{i}f_n^\dagger - f_{n+1}^\dagger\right)\\
\frac{1}{\sqrt{2}\sqrt{1+\alpha_-^2+\beta_-^2}}\left(-\alpha_-(\mathrm{i}d_n^\dagger + d_{n+1}) + \beta_-(\mathrm{i}a_n^\dagger - a_{n+1}^\dagger) + \mathrm{i}f_n^\dagger + f_{n+1}^\dagger\right)\\
\frac{1}{\sqrt{2}\sqrt{1+\alpha_+^2+\beta_+^2}}\left(-\alpha_+(\mathrm{i}d_n^\dagger + d_{n+1}) + \beta_+(\mathrm{i}a_n^\dagger - a_{n+1}^\dagger) + \mathrm{i}f_n^\dagger + f_{n+1}^\dagger\right)
\end{cases} \tag{5.16}$$

where,

$$\begin{aligned} t' &= \frac{2t}{\Delta t_B} + 1, \\ \alpha_{\mp} &= \frac{8t^2 + 8\Delta t_B t \pm 4\sqrt{2}tt'' + 3\Delta t_B^2 \pm 2\sqrt{2}\Delta t_B t''}{\Delta t_B^2}, \\ \beta_{\mp} &= \frac{2\sqrt{2} + \sqrt{2}\Delta t_B \pm 2t''}{\Delta t_B}, \\ t'' &= \sqrt{2t^2 + 2t\Delta t_B + \Delta t_B^2}. \end{aligned} \tag{5.17}$$

The results for $\phi = 0$, calculated using first order perturbation theory, are displayed in table 5.4.

Table 5.1: First order perturbation eigensystem for $\phi = 0$ considering $U = \epsilon_A A_n^\dagger A_n$.

Subspace	Eigenvalue	Eigenvector
1	0 [a]	$a_j^\dagger \left\|0\right\rangle$ [a]
2	$-2\sqrt{2}t\cos(k/2)$	$\frac{1}{\sqrt{2}}\left[\mathrm{e}^{\mathrm{i}(k/4-nk)}d_k^\dagger - \mathrm{e}^{-\mathrm{i}(k/4-nk)}d_{-k}^\dagger\right]\left\|0\right\rangle$
	$-2\sqrt{2}t\cos(k/2) + \epsilon_A/N_c$	$\frac{1}{\sqrt{2}}\left[\mathrm{e}^{\mathrm{i}(k/4-nk)}d_k^\dagger + \mathrm{e}^{-\mathrm{i}(k/4-nk)}d_{-k}^\dagger\right]\left\|0\right\rangle$
3	$2t\cos(k/2)$	$\frac{1}{\sqrt{2}}\left[\mathrm{e}^{\mathrm{i}(k/4-nk)}f_k^\dagger - \mathrm{e}^{-\mathrm{i}(k/4-nk)}f_{-k}^\dagger\right]\left\|0\right\rangle$
	$2t\cos(k/2) + \epsilon_A/N_c$	$\frac{1}{\sqrt{2}}\left[\mathrm{e}^{\mathrm{i}(k/4-nk)}f_k^\dagger + \mathrm{e}^{-\mathrm{i}(k/4-nk)}f_{-k}^\dagger\right]\left\|0\right\rangle$
4	0 [a]	$a_j^\dagger \left\|0\right\rangle$ [a]
	0	$\frac{1}{\sqrt{2}}\left(d_{-\pi}^\dagger - f_{-\pi}^\dagger\right)\left\|0\right\rangle$
	ϵ_A/N_c	$\frac{1}{\sqrt{2}}\left(f_{-\pi}^\dagger + d_{-\pi}^\dagger\right)\left\|0\right\rangle$

[a] Exact result

Table 5.2: First order perturbation eigensystem for $\phi = 0$ considering $U = -\Delta t_A\left(\mathrm{e}^{\mathrm{i}\phi/4}C_n^\dagger A_n + \mathrm{e}^{\mathrm{i}\phi/4}A_n^\dagger B_n + \mathrm{e}^{\mathrm{i}\phi/4}A_n^\dagger C_{n-1} + \mathrm{e}^{\mathrm{i}\phi/4}B_{n-1}^\dagger A_n + \mathrm{h.c.}\right)$.

Subspace	Eigenvalue	Eigenvector
1	0 [a]	$a_j^\dagger \left\|0\right\rangle$ [a]
2	$-2\sqrt{2}t\cos(k/2)$	$\frac{1}{\sqrt{2}}\left[\mathrm{e}^{\mathrm{i}(k/4-nk)}d_k^\dagger - \mathrm{e}^{-\mathrm{i}(k/4-nk)}d_{-k}^\dagger\right]\left\|0\right\rangle$
	$-2\sqrt{2}(t + 2\Delta t_A/N_c)\cos(k/2)$	$\frac{1}{\sqrt{2}}\left[\mathrm{e}^{\mathrm{i}(k/4-nk)}d_k^\dagger + \mathrm{e}^{-\mathrm{i}(k/4-nk)}d_{-k}^\dagger\right]\left\|0\right\rangle$
3	$2\sqrt{2}t\cos(k/2)$	$\frac{1}{\sqrt{2}}\left[\mathrm{e}^{\mathrm{i}(k/4-nk)}f_k^\dagger - \mathrm{e}^{-\mathrm{i}(k/4-nk)}f_{-k}^\dagger\right]\left\|0\right\rangle$
	$2\sqrt{2}(t + 2\Delta t_A/N_c)\cos(k/2)$	$\frac{1}{\sqrt{2}}\left[\mathrm{e}^{\mathrm{i}(k/4-nk)}f_k^\dagger + \mathrm{e}^{-\mathrm{i}(k/4-nk)}f_{-k}^\dagger\right]\left\|0\right\rangle$
4	0 [a]	$a_j^\dagger \left\|0\right\rangle$ [a]
	0	$d_{-\pi}^\dagger \left\|0\right\rangle$
	0	$f_{-\pi}^\dagger \left\|0\right\rangle$

[a] Exact result

Table 5.3: First order perturbation eigensystem for $\phi = 0$ considering $U = \epsilon_B B_n^\dagger B_n$.

Subspace	Eigenvalue	Eigenvector
1	0	$a_{j\neq n}^\dagger \left\|0\right\rangle$
	$\epsilon_B/2$	$a_n^\dagger \left\|0\right\rangle$
2	$-2\sqrt{2}t\cos(k/2)$	$\frac{1}{\sqrt{2}}\left[\mathrm{e}^{\mathrm{i}(k/4+nk)}d_k^\dagger - \mathrm{e}^{-\mathrm{i}(k/4+nk)}d_{-k}^\dagger\right]\left\|0\right\rangle$
	$-2\sqrt{2}t\cos(k/2) + \epsilon_B/2N_c$	$\frac{1}{\sqrt{2}}\left[\mathrm{e}^{\mathrm{i}(k/4+nk)}d_k^\dagger + \mathrm{e}^{-\mathrm{i}(k/4+nk)}d_{-k}^\dagger\right]\left\|0\right\rangle$
3	$+2\sqrt{2}t\cos(k/2)$	$\frac{1}{\sqrt{2}}\left[\mathrm{e}^{\mathrm{i}(k/4+nk)}f_k^\dagger - \mathrm{e}^{-\mathrm{i}(k/4+nk)}f_{-k}^\dagger\right]\left\|0\right\rangle$
	$+2\sqrt{2}t\cos(k/2) + \epsilon_B/2N_c$	$\frac{1}{\sqrt{2}}\left[\mathrm{e}^{\mathrm{i}(k/4+nk)}f_k^\dagger + \mathrm{e}^{-\mathrm{i}(k/4+nk)}f_{-k}^\dagger\right]\left\|0\right\rangle$
4	0	$\frac{1}{\sqrt{N_c+1}}\left[\mathrm{e}^{-\mathrm{i}\pi/4}a_n^\dagger + \frac{\sqrt{2N_c}}{2}\left(d_{-\pi}^\dagger - f_{-\pi}^\dagger\right)\right]$
	0	$\frac{1}{2}\left(d_{-\pi}^\dagger + f_{-\pi}^\dagger\right)$
	$\frac{\epsilon_B+N_c\epsilon_B}{2N_c}$	$\frac{1}{\sqrt{2+2N_c}}\left[\sqrt{2N_c}\mathrm{e}^{-\mathrm{i}\pi/4}a_n^\dagger - \left(d_{-\pi}^\dagger + f_{-\pi}^\dagger\right)\right]$

Table 5.4: First order perturbation eigensystem for $\phi = 0$ considering $U = -\Delta t_B B_n^\dagger \left(\mathrm{e}^{-\mathrm{i}\phi/4}A_n + \mathrm{e}^{\mathrm{i}\phi/4}A_{n+1} + \mathrm{h.c.}\right)$.

	0	$a_j^\dagger \left\|0\right\rangle$
2	$-2t\cos(k/2)$	$\frac{1}{\sqrt{2}}\left[\mathrm{e}^{\mathrm{i}(k/4+nk)}d_k^\dagger - \mathrm{e}^{-\mathrm{i}(k/4+nk)}d_{-k}^\dagger\right]\left\|0\right\rangle$
	$-2\sqrt{2}(t+\Delta t_B/N_c)\cos(k/2)$	$\frac{1}{\sqrt{2}}\left[\mathrm{e}^{\mathrm{i}(k/4+nk)}d_k^\dagger + \mathrm{e}^{-\mathrm{i}(k/4+nk)}d_{-k}^\dagger\right]\left\|0\right\rangle$
3	$2t\cos(k/2)$	$\frac{1}{\sqrt{2}}\left[\mathrm{e}^{\mathrm{i}(k/4+nk)}f_k^\dagger - \mathrm{e}^{-\mathrm{i}(k/4+nk)}f_{-k}^\dagger\right]\left\|0\right\rangle$
	$2\sqrt{2}(t+\Delta t_B/N_c)\cos(k/2)$	$\frac{1}{\sqrt{2}}\left[\mathrm{e}^{\mathrm{i}(k/4+nk)}f_k^\dagger + \mathrm{e}^{-\mathrm{i}(k/4+nk)}f_{-k}^\dagger\right]\left\|0\right\rangle$
4	0	$a_j^\dagger \left\|0\right\rangle$ [a]
	0	$d_{-\pi}^\dagger \left\|0\right\rangle$
	0	$f_{-\pi}^\dagger \left\|0\right\rangle$

5.2 ABC Diamond

Let us now consider the general situation where the A, B and C sites are all different from each other but where we preserve translational symmetry. We can then assume that the hopping amplitude between A and B sites, t_B, is different from that between A and C sites, t_C, and that the on-site energies for A sites, ϵ_A, for B sites, ϵ_B, and for C sites, ϵ_C, are different. We are therefore led to the Hamiltonian,

$$\begin{aligned} H = &-\sum_j t_B \mathrm{e}^{\mathrm{i}\phi/4} A_j^\dagger B_j + t_C \mathrm{e}^{\mathrm{i}\phi/4} C_j^\dagger A_j + t_C \mathrm{e}^{\mathrm{i}\phi/4} A_{j+1}^\dagger C_j + t_B \mathrm{e}^{\mathrm{i}\phi/4} B_j^\dagger A_{j+1} + h.c. \\ &+ \sum_j \epsilon_A A_j^\dagger A_j + \epsilon_B B_j^\dagger B_j + \epsilon_C C_j^\dagger C_j. \end{aligned} \tag{5.18}$$

Due to the translational symmetry it is obvious that this Hamiltonian is easily diagonalizable in Fourier space. The procedure is identical to what we have already done and we are led to the following secular equation,

$$\begin{aligned} &\epsilon_k^3 - \\ &\epsilon_k^2 \left(\epsilon_A + \epsilon_B + \epsilon_C\right) + \\ &\epsilon_k \left(\epsilon_A\epsilon_B + \epsilon_A\epsilon_C + \epsilon_B\epsilon_C - 4t_B^2 \cos^2\left(\phi/4 + k/2\right) - 4t_C^2 \cos^2\left(\phi/4 - k/2\right)\right) + \\ &4t_B^2 \cos^2\left(\phi/4 + k/2\right)\epsilon_C + 4t_C^2 \cos^2\left(\phi/4 - k/2\right)\epsilon_C - \epsilon_A\epsilon_B\epsilon_C = 0. \end{aligned} \tag{5.19}$$

In some situations a simple solution can be found. When we have $t_B = 0$ (or identically, $t_C = 0$), the Hamiltonian reduces to that of quantum ring of $2N_c$ threaded by a flux $N_c\phi/2$ plus N_c independent sites. The eigenvalues are,

$$\epsilon_k = \epsilon_B, \pm\sqrt{\frac{\left(\epsilon_A - \epsilon_C\right)^2}{2} + 2t_C^2 + 2t_C^2\cos(k - \phi/2) + \epsilon_C}. \tag{5.20}$$

and the eigenstates are simply extended plane waves for the sites belonging to the ring and one site localized states for the independent sites. If we make instead $t_C = 0$, the solution is the same provided we make the substitution,

$$\begin{Bmatrix} B_j \\ C_j \\ \phi \\ t_B, \epsilon_B \\ t_C, \epsilon_C \end{Bmatrix} \rightarrow \begin{Bmatrix} C_j \\ B_j \\ -\phi \\ t_C, \epsilon_C \\ t_B, \epsilon_B \end{Bmatrix}. \tag{5.21}$$

Another simple solution can be found if we make instead $\epsilon_B = \epsilon_C = 0$, the spectrum of the system being given in this case by,

$$\epsilon_k = 0, \sqrt{\left(\frac{\epsilon_A}{2}\right)^2 + 2t_B^2 + 2t_C^2 + 2t_B^2\cos\left(k + \phi/2\right) + 2t_C^2\cos\left(k - \phi/2\right)} + \epsilon_A. \tag{5.22}$$

If we assume the B and C sites to be identical, not only $\epsilon_B = \epsilon_C$ as we have done, but we also have $t_B = t_C = t$,[1] the spectrum of the system reducing to,

$$\epsilon_k = 0, \pm 2t\sqrt{1 + \cos(k)\cos(\phi/2) + \left(\frac{\epsilon_A}{4t}\right)^2} + \epsilon_A. \tag{5.23}$$

The different on-site energies of the A and B and C sites open a gap in the dispersion relation for $\phi = 0$ as could be anticipated. Also, by shifting the top and bottom band, it can cause band

[1] Assuming that the geometry is such that the overlap between A and B atoms is equal to that between A and C atoms.

crossing[2] as depicted in Fig. 5.1. By making $\epsilon_A/t \gg 1$ the bands tend to become flat since we force the localization of the wavefunction preventing transport in the system. Note that, independently of the value of ϵ_A, the top and bottom band states with momentum $k = \pm\pi/2$ have an energy that does not depend on the flux.

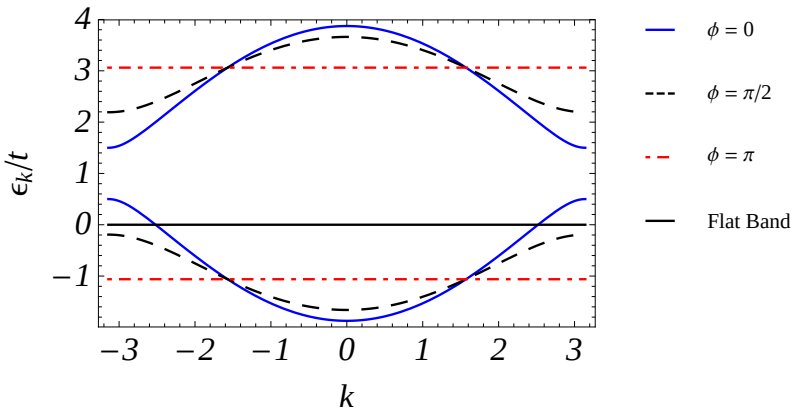

Figure 5.1: Dispersion relation for $\epsilon_B = \epsilon_C = 0$, $\epsilon_A = t_B = t_C = t$. Note the gap for $\phi = 0$, absent when $\epsilon_A = 0$ and the band crossing. Note also that the top and bottom band states with $k = \pm\pi/2$ have and energy independent of the flux.

Let us now examine the gaps and the bandwidth in this particular situation. Let us divide the system in three regimes according to the value of ϵ_A, in order of its increasing absolute value (see Fig. 5.2):

1. Before the bottom (for $\epsilon_A > 0$)/top (for $\epsilon_A < 0$) band intercepts the middle band.
2. While the bottom/top band is intercepting the bottom band.
3. After the bottom/top band has completely crossed the middle band and exchanged positions.

Let ϵ_A^j denote the values of ϵ_A for which regime j is valid. We then have,

$$\begin{aligned} \sqrt{\frac{3}{2}}\frac{|\epsilon_A^1|}{4t} &\leq |\sin(\phi/4)|, \\ |\sin(\phi/4)| \leq \sqrt{\frac{3}{2}}\frac{|\epsilon_A^2|}{4t} &\leq |\cos(\phi/4)|, \\ \sqrt{\frac{3}{2}}\frac{|\epsilon_A^3|}{4t} &\geq |\cos(\phi/4)|. \end{aligned} \tag{5.24}$$

For regime 1, the top-middle band gap ΔE_{tm}, the middle-bottom band gap ΔE_{mb} and the total bandwidth W are,

$$\begin{aligned} \Delta E_{tm} &= 2t\sqrt{2\sin^2(\phi/4) + (\epsilon_A/4t)^2} + \epsilon_A, \\ \Delta E_{mb} &= 2t\sqrt{2\sin^2(\phi/4) + (\epsilon_A/4t)^2} - \epsilon_A, \\ W &= 4t\sqrt{2\cos^2(\phi/4) + (\epsilon_A/4t)^2}. \end{aligned} \tag{5.25}$$

[2]Despite this crossing we will continue to refer to d_k band as the bottom band, to the a_k band as the middle band and to the f_k band as the top band.

For regime 2 we have only one band gap, between the top and bottom bands, ΔE_{tb},

$$\Delta E_{tb} = 4t\sqrt{2\sin^2(\phi/4) + (\epsilon_A/2t)^2}, \tag{5.26}$$

while the bandwidth of the system is given by the same expression as in regime 1. Finally, for regime 3 we have two band gaps, one between the bottom and top which is equal to that of regime 2, the other between the bottom and middle bands ΔE_{bm} (or middle and top bands if $\epsilon_A < 0$. In that case we have $\Delta E_{mt} = -\Delta E_{bm}$). The expression for the bandwidth of the system W' is now different from previous regimes. One has in this regime,

$$\begin{aligned} \Delta E_{bm} &= 2t\sqrt{2\cos^2(\phi/4) + (\epsilon_A/2t)^2} - \epsilon_A, \\ W' &= 2t\sqrt{2\sin^2(\phi/4) + (\epsilon_A/4t)^2} + \epsilon_A. \end{aligned} \tag{5.27}$$

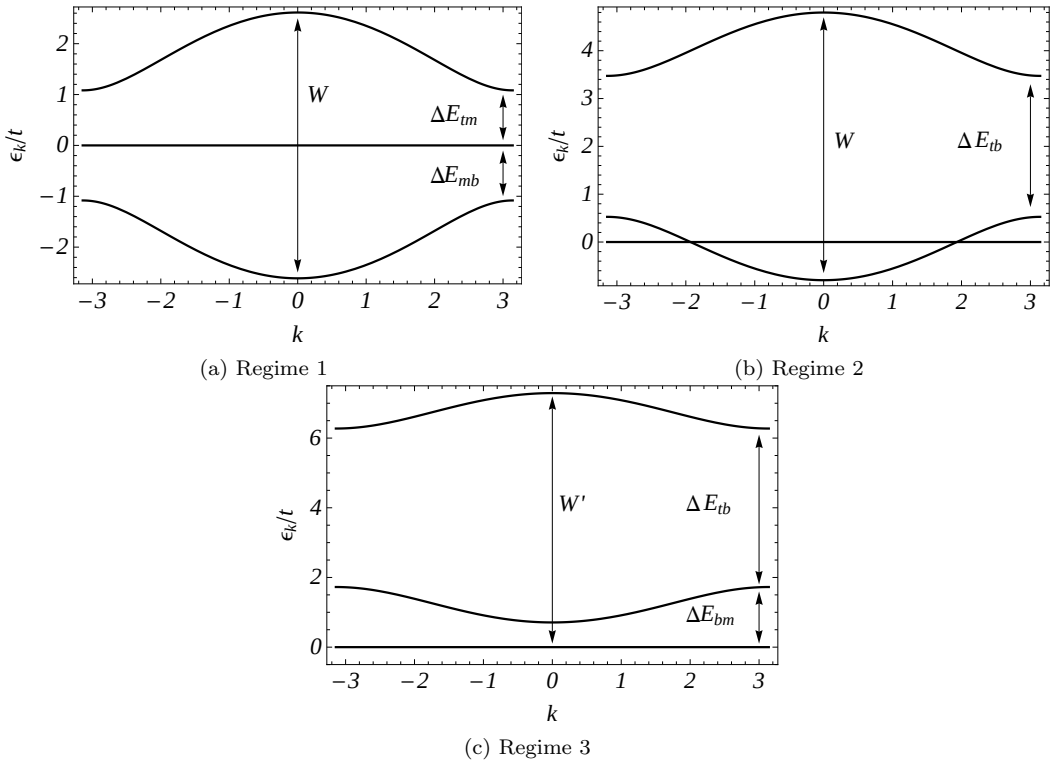

(a) Regime 1

(b) Regime 2

(c) Regime 3

Figure 5.2: The three regimes of the studied system, here considering $\epsilon_A > 0$. The three regimes are distinguished by the relative position of the energy bands.

Chapter 6

Interactions in the diamond chain

In this chapter we address the effect of interactions in the diamond chain. Interactions lead to many interesting phenomena and are responsible for fascinating physics. One remarkable example is superconductivity. Without interactions there are no correlation effects and the possibility of ordered phases as we see in nature is non-existent. We will limit ourselves to the study of interactions using a mean field approach altough interactions will also be considered on the next chapter when dealing with the conductance of our chain. We will be considering two types of interactions. For a system with spin we will consider a Hubbard like interaction consisting of an on-site Coulomb interaction between opposing spins,

$$H = H_0 + U \sum_{j}^{N_c} n^A_{j,\uparrow} n^A_{j,\downarrow} + n^B_{j,\uparrow} n^B_{j,\downarrow} + n^C_{j,\uparrow} n^C_{j,\downarrow}, \tag{6.1}$$

where H_0 is the tight binding Hamiltonian of Eq. (2.21), including spin, $n_j = c^\dagger_j c_j$ is the particle number operator and U is the value of the interaction. This Hubbard interaction is generally the dominant interaction term in most systems and the Hubbard model present us with very interesting physics. Despite its simplicity it is still not fully understood. [19] For a spinless system, we will consider what is often the dominant interaction, a Coulomb like interaction between nearest neighbors,

$$H = H_0 + V \sum n^A_j n^B_j + n^A_{j+1} n^B_j + n^A_j n^C_j + n^A_{j+1} n^C_j, \tag{6.2}$$

where V is the value of the interaction, here assumed to be isotropic. We call this the t-V model. We assume that due to screening the interaction between second nearest neighbors is very small and therefore that it can be neglected.[1] Such spinless system does not mean that spin is non existent, but simply that it is not an available degree of freedom. Such state can be obtained by polarizing the system using an external magnetic field, or because the Hubbard interaction induces a ferromagnetic state.

The highly degenerate flat band states present in the diamond chain mean that any interaction is effectively a strong interaction even if the interaction energy is small compared with the hopping amplitude. This provides us an experimental testing ground to study the strong coupling limit even if the interactions present on the system are weak.

Mean field (MF) theory allows us to turn an Hamiltonian containing two body interactions into a quadratic Hamiltonian in the creation and annihilation operators, i.e., into an effective Hamiltonian not containing interactions. Although the MF theory tends to produce uncontrolled results, showing phase transitions where they don't occur being a particular bad approximation for low dimensional system such as ours, it is nevertheless an easy approximation to make which allow us to gain some insight into our system.

[1] One could suppose, that since Coulomb potential falls with the inverse of the distance between the particles we could neglect second neighbors interaction using this argument. However, assuming a 1D periodic lattice with one electron per unit cell, we have that the interaction between nearest neighbors is proportional to e^2/a while between next nearest neighbors is proportional to $e^2/(2a)$. Obviously, $1/2 \not\ll 1$ and therefore the argument fails. Screening however, can reduce the interaction dramatically.

6.1 On-site Coulomb repulsion

We will begin by concerning ourselves with a Hubbard interaction and treating it using MF theory. The operator number of particles can be written as its average plus the deviation from the average,

$$n_{j\sigma} = \overline{n}_{j\sigma} + (n_{j\sigma} - \overline{n}_{j\sigma})\,. \tag{6.3}$$

Using this expression we make the approximation,

$$n_{j\uparrow}n_{j\downarrow} \approx n_{j\uparrow}\overline{n}_{j\downarrow} + n_{j\downarrow}\overline{n}_{j\uparrow} - \overline{n}_{j\uparrow}\overline{n}_{j\downarrow}, \tag{6.4}$$

and the interaction term can be written as

$$H_{int} = U\sum_j \left(n^X_{j\uparrow}\overline{n}^X_{j\uparrow} + n^X_{j\downarrow}\overline{n}^X_{j\downarrow} - \overline{n}^X_{j\uparrow}\overline{n}^X_{j\downarrow}\right), \quad X = A, B, C. \tag{6.5}$$

We will begin by assuming that the density of particles with spin σ is uniform on A, B and C sites and assume it to be identical for B and C sites,

$$\begin{aligned} \overline{n}^A_\sigma &= \overline{n}^A_{j\sigma}, \\ \overline{n}^B_\sigma &= \overline{n}^B_{j\sigma} = \overline{n}^C_{j\sigma}. \end{aligned} \tag{6.6}$$

This restriction still allow us to study ferromagnetic, antiferromagnetic and ferrimagnetic configurations due to the bipartite nature of the diamond chain. The MF energy dispersion relation of our system will be the roots of a secular equation identical to Eq. (5.19) and no simple expression exists for general ϕ. However for $\phi = 0$ a simple expression exists for the MF dispersion relation (ignoring the constant term in Eq. (6.5)),

$$\begin{aligned} \epsilon^{\text{flat}}_\sigma &= U\overline{n}^B_{-\sigma} \\ \epsilon^{\pm}_\sigma &= \frac{1}{2}\left[U\left(\overline{n}^A_{-\sigma} + \overline{n}^B_{-\sigma}\right) \pm \sqrt{\Delta^2_{-\sigma} + 32t^2\cos^2(k/2)}\right], \end{aligned} \tag{6.7}$$

where,

$$\Delta_{-\sigma} = U\left(\overline{n}^A_{-\sigma} - \overline{n}^B_{-\sigma}\right). \tag{6.8}$$

corresponding to one localized state and two dispersive states.

6.1.1 Ferromagnetic ordering

In order to study ferromagnetic ordering we will assume that the average density of up and down spins of our system is different but uniform,

$$\overline{n}_\sigma = \overline{n}^A_{j\sigma} = \overline{n}^B_{j\sigma} = \overline{n}^C_{j\sigma}, \tag{6.9}$$

where $\overline{n}_\sigma$ is the density of spin σ of the system. For the sake of simplicity we will assume that we are working on a canonical ensemble. The total density of particles of our system is then,

$$\overline{n} = \overline{n}_\uparrow + \overline{n}_\downarrow = \frac{N_p}{N_s}, \tag{6.10}$$

where N_p is the number of particles of our system and N_s the number of sites. To find the multiparticle energy at zero temperature, one just needs to fill the single particle levels from the lowest to the highest taking into account Pauli's exclusion principle.

We define the magnetization of the system as,

$$m = \frac{\overline{n}_\uparrow - \overline{n}_\downarrow}{\overline{n}_\uparrow + \overline{n}_\downarrow} \in [-1, 1]. \tag{6.11}$$

By calculating the multiparticle energy, E, as a function of the magnetization, one can find the ground state of the system. It is given by the magnetization that minimizes the energy (or free

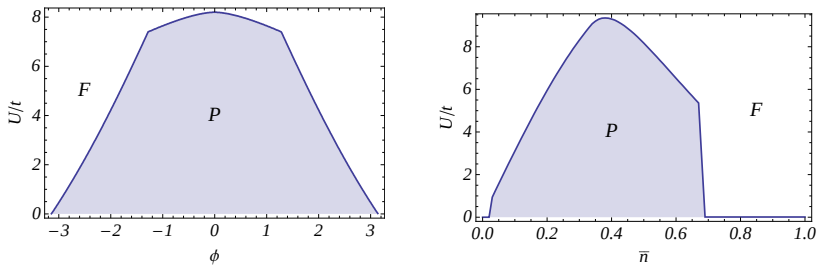

(a) As function of flux at half filling (b) As function of filling

Figure 6.1: The phase transition between paramagnetic and ferromagnetic order for a system with 128 (a), and 300 (b) cells obtained by studying MF ferromagnetic ordering. In (b) we only plot until $\overline{n} = 1$ since the graphic is even around $\overline{n} = 1$.

energy if one works on a grand-canonical ensemble). One thing to note is that $E(m)$ is even in m, since going from negative to positive m just means that the up and down spins have exchanged their role. By numerically filling the energy levels for several values of magnetization, we computed the phase transition curve between the ferromagnetic phase and paramagnetic phase of the diamond chain. The phase diagram as a function of flux is given in Fig. 6.1a for a filling of $\overline{n} = 0.5$ (quarter filling) and as a function of the filling in Fig. 6.1b for $\phi = 0$. One must note that the obtained phase transitions are in accordance with Stoner's criterion,

$$U_c = \frac{1}{D(\epsilon_F)}, \tag{6.12}$$

where U_c is the value of the interaction for which the phase transition between paramagnetic and ferromagnetic states occurs and $D(\epsilon_F)$ is the DOS at the Fermi level. In our system, we have a flat band, whose DOS diverges. The flat band starts to fill up when the lower band is completely full. This happens when one has a filling of one third the maximum filling, $\overline{n} = 2/3$. The flat band is completely filled when we have a filling of two thirds of the maximum filling, $\overline{n} = 4/3$ and according to Stoner's criterion we expect that $U_c = 0$ in this interval which is indeed observed in our MF results.

6.1.2 Antiferromagnetic ordering

Let us now study antiferromagnetic ordering in our system. In an antiferromagnetic ordering, nearest neighbor sites have an alternating mean excess of up/down spins. We also require the total (mean) magnetization of our system to be zero. We therefore assume that A sites have an excess of up spin while B and C sites have an excess of down spin and that the average density of up/down spins only depend on the type of site (i.e. A, B or C). We therefore have,

$$\begin{aligned} \overline{n}_\sigma^A &= \overline{n}_{j\sigma}^A, \\ \overline{n}_\sigma^B = \overline{n}_{j\sigma}^B &= \overline{n}_{j\sigma}^C, \\ \overline{n}_\sigma^A &= 2\overline{n}_{-\sigma}^B, \end{aligned} \tag{6.13}$$

so that the total density of particles is given by (considering that we have three sites per unit cell),

$$\overline{n} = \frac{2\overline{n}_A}{3}, \tag{6.14}$$

where $\overline{n}_A = \overline{n}_\uparrow^A + \overline{n}_\downarrow^A$.

We define staggered magnetization as

$$m_S = \frac{\overline{n}_\uparrow^A - \overline{n}_\downarrow^A}{\overline{n}_\uparrow^A + \overline{n}_\downarrow^A}, \tag{6.15}$$

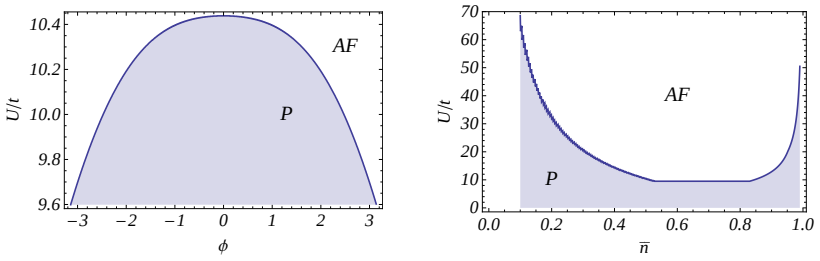

(a) As function of flux at half filling

(b) As function of filling

Figure 6.2: The phase transition between paramagnetic and antiferromagnetic order for a system with 128 cells obtained by studying MF antiferromagnetic ordering. We only plot until $\overline{n} = 1$ since the graphic is even around $\overline{n} = 1$.

and in order to calculate the phase diagram of the system we will iterate over the allowed values of m_S. Obviously, paramagnetic ordering occurs for $m_S = 0$. We calculated the phase diagram between paramagnetic and antiferromagnetic ordering as a function of flux and filling Fig. 6.2.

We also compared the results of ferromagnetic and antiferromagnetic ordering, and concluded that antiferromagnetic ordering always loses, i.e., the energy of the paramagnetic/ferromagnetic order is always lower. Our system appears therefore to not exhibit antiferromagnetism, at least in MF. The number of unit cells used in the numerical calculations was always (unless otherwise stated) $Nc = 128$ which correspond to 384 sites. This value was chosen since it was seen that, for that number of cells, the energy of the system per unit cell did not change significantly with increasing number of cells, so that finite size effects should not be significant.

That the ferromagnetic state should be lower in energy than the antiferromagnetic has been observed by Macêdo et al., [11] and at least at half filling the system is in fact ferrimagnetic. It is also known that if the lowest band is flat, a condition we can force as discussed in previous chapter, the ground state should be ferromagnetic. [20]

6.2 Nearest neighbors Coulomb interaction

When considering nearest neighbors Coulomb interaction we will be interested on the density of particles on A, B and C sites. We assume the particle density on site X to be the average number of particles per number of unit cell, $\overline{n}_X = \overline{N}_X/N_c$ We also assume that the particle density on B and C sites is the same, which is justified since they are related by a symmetry operation. Let $\overline{n}$ denote the total particle density, $\overline{n} = N_p/N_s$,

$$\overline{n} = \frac{\overline{n}_A + 2\overline{n}_B}{3}, \tag{6.16}$$

where $\overline{n}_A$ and $\overline{n}_B$ are the particle densities in A and B sites respectively per unit cell. We then have,

$$0 < \left\{ \begin{matrix} \overline{n} \\ \overline{n}_A \\ \overline{n}_B \end{matrix} \right\} < 1. \tag{6.17}$$

In this situation, the interaction part of the MF Hamiltonian can be written as,

$$H_{int} = 2V \sum_j \left[2\overline{n}_B n_j^A + \overline{n}_A n_j^B + \overline{n}_A n_j^C \right] - 2N_c \overline{n}_A \overline{n}_B. \tag{6.18}$$

While there is no simple expression for the MF dispersion relation for general ϕ, a simple expression exists for zero flux,

$$\begin{aligned} \epsilon_\sigma^{\text{flat}} &= 2V\overline{n}_A \\ \epsilon_\sigma^{\pm} &= V\left(\overline{n}_A + 2\overline{n}_B\right) \pm \sqrt{8t^2\cos(k/2) + \Delta_V^2}, \end{aligned} \tag{6.19}$$

where $\Delta_V = V(\overline{n}_A - 2\overline{n}_B)$. Let us therefore examine this simpler situation. We define the order parameter as the excess of density on the A sites,

$$\Delta\overline{n} = \frac{\overline{n}_A - 2\overline{n}_B}{\overline{n}_A + 2\overline{n}_B}. \tag{6.20}$$

Due to the equivalence of the B and C sites, we regard our system as being a dimerized system consisting of two alternating types of pseudo-sites: A sites and BC pseudo-sites. Note however that this picture is to be interpreted with caution since BC pseudo-sites are not real sites and can take twice as many electrons as the A sites. One must note that in a general situation we have $\Delta\overline{n} \in [-1, 1]$ but since we must have $0 < \overline{n}_A, \overline{n}_B < 1$, we have that for $\overline{n} > 1/3$ $\Delta\overline{n}$ is limited to the interval $[-1, \Delta\overline{n}_{\max}]$, where $\Delta\overline{n}_{\max}$ lies in $[0, 1]$ and whose value decreases with increasing $\overline{n}$. For the same reason, for $\overline{n} = 2/3$ we have that $\Delta\overline{n}$ is limited to $[-1, 0]$ and for $\overline{n} > 2/3$ not only the upper limit of $\Delta\overline{n}$ decreases with increasing $\overline{n}$ but also the lower limit of $\Delta\overline{n}$ increases with increasing $\overline{n}$. For $\overline{n} = 1$ we have $\Delta\overline{n} = -1/3$, corresponding to an equal density of particles on every site, the only possible state when the system is completely filled. The phase diagram of the system is depicted in Fig. 6.3. We note that we can have a uniform density phase that can exist only for a filling $\overline{n} < 1/3$ and that in this region, starting in the uniform density phase, by increasing the interaction we are able to localize an excess of electron density on A sites or on BC pseudo-sites, both situation being symmetric. By further increasing the interaction we are able localize all the electrons on A sites or on BC pseudo-sites where both situations remain symmetric. In the region $1/3 < \overline{n} < 2/3$ the uniform density phase would require $\overline{n}_A > 1$ which is forbidden by Pauli's exclusion principle and therefore that phase is innexistent in that interval of filling. We also note that we no longer can localize the full electrons density on A sites while we can on BC sites and therefore although the Hamiltonian treats A and BC pseudo-sites equally, the Pauli's exclusion breaks the symmetry between A and BC pseudo-sites, lowering the symmetry of the system. In the region $\overline{n} > 2/3$, again due to Pauli's exclusion principle, we are not able to fully localize the density of electrons even on BC pseudo-sites and only one phase remains.

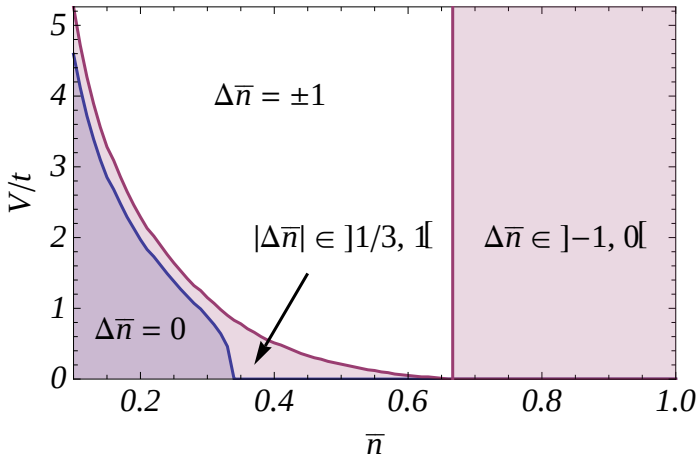

Figure 6.3: MF phase diagram for the spinless diamond chain considering a nearest neighbors Coulomb interaction and $N_c = 128$. For $\overline{n} < 1/3$ we can have a uniform density phase, a phase with excess of density on A or BC pseudo-sites and a phase where all the density of particles is situated on A or BC pseudo-sites. For $\overline{n} > 1/3$ Pauli's exclusion principle breaks the symmetry between A and BC pseudo-sites; a uniform density phase is not possible anymore and the density of particles can no longer be situated only on A sites. It can however, for $\overline{n} < 2/3$, be situated only on BC pseudo-sites. For $\overline{n}$, due to Pauli's exclusion principle, the density of particles is required to be spread among A and BC sites and for $\overline{n} = 1$ the order parameter is $\Delta\overline{n} = -1/3$, which implies a uniform density of particles between the real A,B and C sites.

Chapter 7

Conductance

In this chapter we address the phenomena of coherent transport through the diamond. We follow the approach of Balseiro et al. by [21] considering discrete tight binding leads weakly coupled to our system. We start by treating the non-interacting diamond star and later introduce a nearest neighbors Coulomb interaction comparing both results.

7.1 Conductance in the diamond star

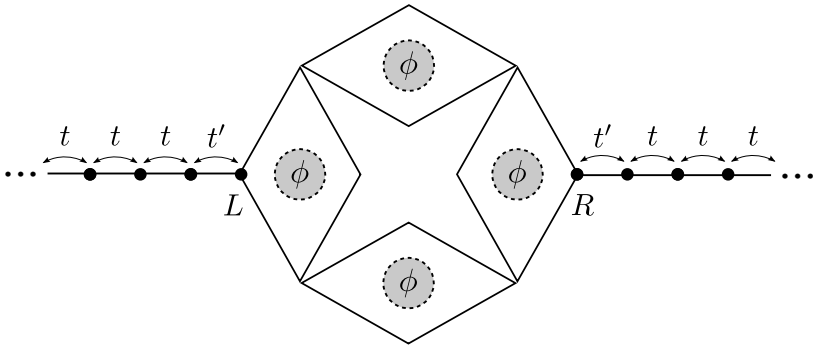

Figure 7.1: In this chapter we consider the diamond star to be connected, at sites L and R, to semi-infinite tight binding leads via a hopping amplitude t'. The hopping amplitude of the leads is taken to be the same to that of the star, t.

Let us consider the diamond star discussed in chapter 4 with sites L and R connected to left and right leads respectively. We consider these leads to be described by a tight binding model and to be weakly coupled to our star as depicted in Fig. 7.1. The Hamiltonian of the full system is given by,

$$H_{star} + H_{leads} + H_{hyb} \tag{7.1}$$

where H_{star} is the Hamiltonian of the isolated diamond star, Eq. (2.21), H_{leads} is the Hamiltonian of the isolated leads, assumed to be semi-infinite,

$$H_{leads} = -t \sum_{j=1,\sigma}^{\infty} a^{\dagger}_{j,\sigma} a_{j+1,\sigma} + a^{\dagger}_{-j-1,\sigma} a_{-j,\sigma} + \text{h.c.}, \tag{7.2}$$

and where we assumed, for simplicity, the hopping amplitude in the leads to be the same to that of the star. H_{hyb} is the hybridization between the diamond star and the leads,

$$H_{hyb} = -t' \sum_{\sigma} a^{\dagger}_{-1,\sigma} c_{L,\sigma} + a^{\dagger}_{1,\sigma} c_{R,\sigma} + \text{h.c.} \tag{7.3}$$

where t' is a small hopping amplitude coupling the leads and the star and $c^{\dagger}_{L,\sigma}$ and $c^{\dagger}_{R,\sigma}$ create an

electron on site L and R, respectively, of the diamond star according to,

$$\begin{aligned} A_j^\dagger &= c_{3j-2}^\dagger \\ B_j^\dagger &= c_{3j-1}^\dagger \\ C_j^\dagger &= c_{3j}^\dagger \end{aligned} \tag{7.4}$$

as depicted in Fig. 7.2. In this situation as studied by Balseiro et al. [21] for 1D quantum rings, the

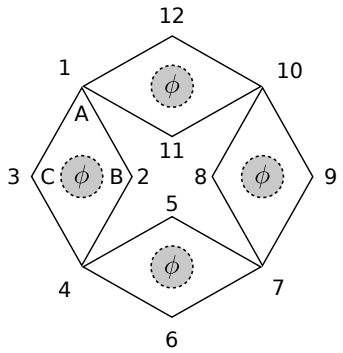

Figure 7.2: The numeration used for the diamond star.

transmittance of the system to an incident particle with momentum k and energy $\omega = -2t\cos(k)$ is,

$$T = \frac{4t^2 \sin^2(k) \left|\tilde{t}(\omega)\right|^2}{\left|\left[\omega - \epsilon(\omega) + t\mathrm{e}^{\mathrm{i}k}\right]^2 - \left|\tilde{t}(\omega)\right|^2\right|} \tag{7.5}$$

where,

$$\begin{aligned} \epsilon(\omega) &= t'^2 G_{LL}^R(\omega) \\ \tilde{t}(\omega) &= t'^2 G_{LR}^R(\omega) \end{aligned} \tag{7.6}$$

represent a correction to the hybridized hopping amplitude and to the on-site energy of the sites connected to the leads. G_{LL}^R and G_{LL}^R are retarded Greens functions in momentum space given by,

$$G_{LR}^R(\omega) = \sum_e \frac{\langle g| c_{R\sigma}^\dagger |e\rangle \langle e| c_{L\sigma} |g\rangle}{\omega + E_e - E_g} \tag{7.7}$$

where $|g\rangle$ and E_g are respectively the ground state and ground energy of the initial system (before we propagate a particle through the system) and $|e\rangle$ and E_e are the states and respective energies of the intermediate system (the initial system plus the particle). We will assume, withouth loss of generality, that a hole is propagating through our system such that the initial system has N electrons and the intermediate one $N-1$. Introducing a gate voltage in our system amounts to sum a constant term to the Hamiltonian, $H \to H - eV_gN$ and this can be taken in account by modifying the denominator of the Green's functions according to, $\omega + E_e - E_g \to \omega + E_e - E_g + eV_g$, where $E_e = E_e^{N-1}$ and $E_g = E_g^N$. The conductance in our coherent system is simply given by Landauer's formula,

$$G = \frac{ne^2}{h} T \tag{7.8}$$

where n is related to the degeneracies of the system. Therefore if we know the transmittance of a particle through our system then we know its conductance. The transmittance/conductance will show peaks at specific values of the gate voltage. Those peaks are located at $E_e^{N-1} = E_g^N + eV_g$ provided the corresponding matrix elements in Eq. (7.7) are non zero. There will in general

exist several peaks as the gate voltage is varied corresponding to the crossing of the ground state of the initial N particles system and the states of the intermediate $N-1$ particles system. The conductance for a one dimensional quantum ring has been thoroughly studied and is well understood. By changing the position of the leads it is possible to change the behavior of the system. However the diamond star offers greater complexity than a simple 1D quantum ring and we can have very different conductance behaviors depending on the position of the leads. Fig. 7.3 shows the difference between positioning the leads at positions 1 and 7, i.e. on A sites two cells apart, and 2 and 3, i.e. on a B and a C site belonging to the same cell for a non-interacting star and considering $N_c = 4$, $N = 3$, $t' = 0.1t$. When we position the leads on sites 2 and 3 we have a ring like topology and the results are identical to what is observed for non interacting quantum rings, the height of the peaks depending on the flux. [22] When $\phi \to \pi$, the negative interference between the waves travelling through both sides of the ring suppresses the transmittance and consequently the conductance of a particle through the system. On the other hand, when we position the leads at sites 1 and 7 we no longer preserve the topology of a ring and it is seen that the transmittance, when considering a coupling between the ground state energies of the N and $N-1$ particle systems, is unitary for any value of flux except $\phi \to \pi$ where it falls to zero. We also note that in both cases we have several peaks situated at $E = -4t$ corresponding to flux independent excited eigenstates of the intermediate $N-1$ particles systems as depicted in Fig. 7.5. However as pointed out by Rincon et al. [22] these peaks should not be accessible experimentally. When we introduce a nearest neighbors Coulomb interaction, $V = 0.5$, in our system, it is seen that when we position the leads at sites $L = 1, R = 7$ the only effect of the interaction is to shift the position of the peaks. No peak is observed for $\phi = \pi$. However, for $L = 2, R = 3$ not only is the position of the peaks affected but we can also see a peak for $\phi = \pi$ as shown in Fig. 7.4.

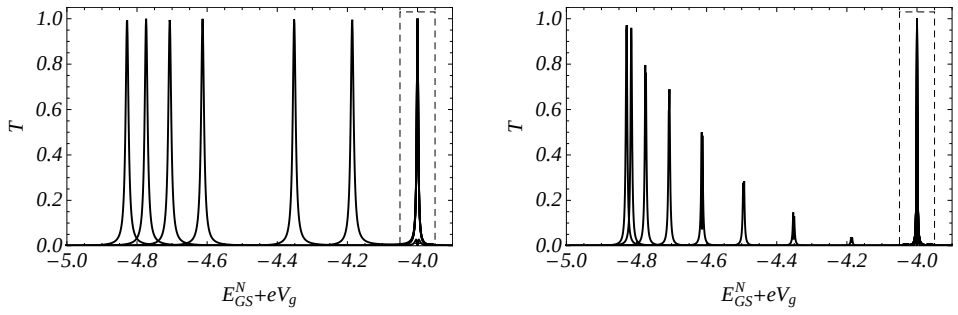

(a) $L = 1$,$R = 7$ (b) $L = 2$,$R = 3$

Figure 7.3: Transmittance peaks as function of the difference between the N particle ground state energy and the gate energy for a diamond star with $N_c = 4$ and $N = 3$ and two distinct leads positions. The coupling between the leads and the star was taken to be $t' = 0.1t$. The unboxed peaks correspond to the coupling between the ground states of the N and $N-1$ particles systems for several values of flux. From left to right these are, $\phi = 0, \pi/8, \pi/4, 3\pi/8, \pi/2, 5\pi/8, 3\pi/4, 7\pi/8$. No peak is observed for $\phi = \pi$. The boxed peaks correspond to the coupling between the ground state of the N particles system and the first excited state of the $N-1$ particles system which is flux independent. We note that these excited peaks should not be achievable experimentally as pointed by Rincon et al. [22] For $L = 1, R = 7$ the values of the peaks are independent of the flux while for $L = 2, R = 3$ they are flux dependent, in accordance to what happens in quantum rings [22].

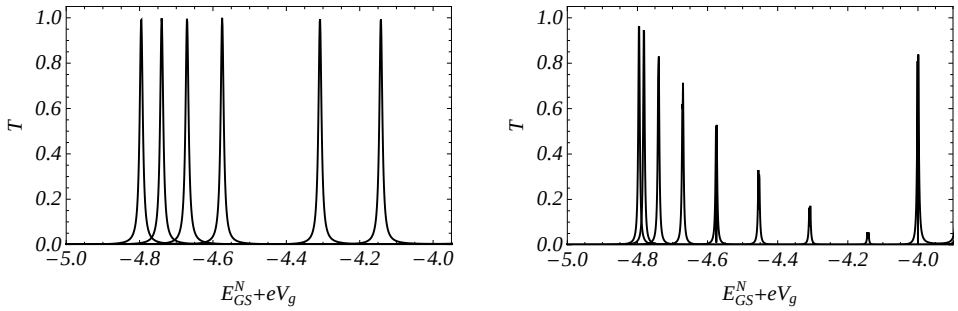

(a) $L = 1$,$R = 7$ (b) $L = 2$,$R = 3$

Figure 7.4: Transmittance peaks as function of the the gate energy for a diamond star with nearest neighbors Coulomb interaction, $V = 0.5t$, $N_c = 4$ and $N = 3$ and two distinct leads positions. The coupling between the leads and the star was taken to be $t' = 0.1t$. The shown peaks correspond to the coupling between the ground states of the N and $N-1$ particles systems for several values of flux. From left to right these are, $\phi = \phi = 0, \pi/8, \pi/4, 3\pi/8, \pi/2, 5\pi/8, 3\pi/4, 7\pi/8, \pi$. Like in the non interacting case when $L = 1, R = 7$ no peak is observed for $\phi = \pi$ and the interaction only shifts the position of the peaks. On the other hand, when $L = 2, R = 3$ the peaks are not only shifted but the point of zero conductance no longer occurs for $\phi = \pi$ and a peak is seen for $\phi = \pi$ at $E^{N-1}_{G.S} = -4t$.

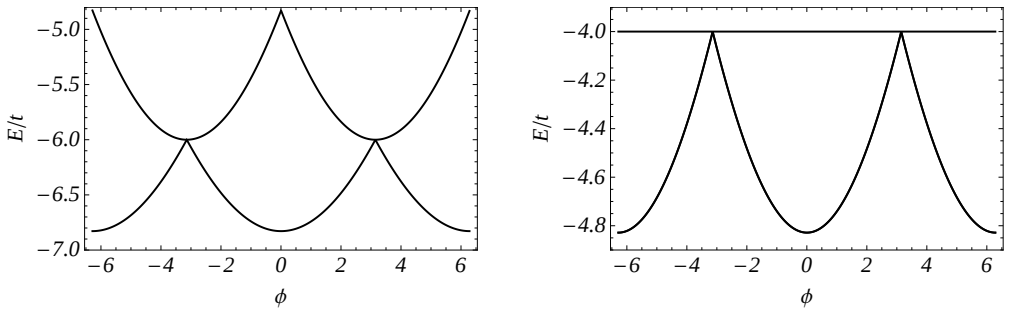

(a) $N_c = 4, N = 3$ (b) $N_c = 4, N = 2$

Figure 7.5: The two lowest distinct eigenvalues as a function of the flux for two $N_c = 4$ systems with number of particles differing by unit. Note that when $N = 2$ there is a flux independent eigenvalue.

Conclusions and future work

The diamond chain is indeed an extraordinary system with many interesting properties. It is a quasi one dimensional system consisting of several rings allowing one to introduce a Peierls phase in the system via an external magnetic flux and to observe the Aharonov-Bohm effect. This system exhibits a flat, dispersionless band for any value of magnetic flux which is quite interesting in such low dimensional system. The diamond chain can be used to describe linear systems such as metal ligand complexes or molecular structures with ring like geometries relevant for molecular electronics. Given current nanofabrication technology it should also be possible to synthesize diamond chain like structures. The possible applications of the diamond chain concern areas such as quantum information systems and logic gate fabrication among others. For a zero magnetic flux electrons in a diamond chain can behave like Dirac particles near one third and two thirds filling. We have demonstrated that in a finite system the periodicity of the properties of the diamond chain on the magnetic flux depend on the parity of the number of unit cells which is indeed relevant for molecular systems. When the magnetic flux is zero or equal to half the quantum of flux, we can have a localized energy eigenbasis. We have also done a mapping of the diamond chain onto a periodic Anderson like model which brings a different interpretation of the diamond chain. We have shown that the addition of hops between next nearest neighbors allow the flat band to become dispersive and these hops can even be used to tune the sign of the effective mass of the electrons. We have also studied the effect of adding an impurity to the chain for the specific cases of zero flux and half quantum of flux flux, which lifts some degeneracies in our system. The effect of the impurity in localized states was seen to be independent of the size of the system while its effect in completely delocalized states decreases when one increases the size of the system. We have also seen how, by making the sites of the unit cell different from each other, the ABC chain, we can control the position of the flat band, the number of gaps on the system, the width of such gaps and the bandwidth of the system, important properties for electronic applications.

Interactions were studied using MF theory for a Hubbard like interaction and for interacting spinless fermions. For the Hubbard like interaction we confirmed previous results while for interacting spinless fermions we have obtained new results and shown that the diamond chain shows an interesting phase diagram and behavior due to Pauli's exclusion principle. We also investigated the conductance of a hole through our system. The greater complexity of the diamond star when compared to a 1D quantum ring means that we can have very different behaviors depending on the position of the leads.

In the future we would like to investigate analytically the effect of interactions on the flat band, using the strong coupling limit formalism for the Hubbard model and for interacting spinless fermions. We are also interested in studying other systems showing flat bands and others macroscopic degeneracies and to treat the conductance through the diamond star in a more detailed and rigorous approach. We are strongly convined that the study of the diamond chain can be easily extrapolated to higher dimensional systems and to rings containing a different number of sites, like benzene based compounds, commonly found in nature.

Appendix A

Thermodynamics of a single mode fermionic oscillator

The fermionic oscillator is so called because of the its similarity with the bosonic harmonic oscillator. It is defined as a single site in momentum space [1],

$$H = \epsilon_k c_k^\dagger c_k. \tag{A.1}$$

Only two states are possible, or we have no particles in the system, or we have a single particle with momentum k. Therefore the grand canonical partition function is trivially,

$$Z = \mathrm{e}^{-\beta(\epsilon_k - \mu)} + 1. \tag{A.2}$$

Since we only have one energy level, the dependence on μ is always identical to the dependence on ϵ for all the thermodynamic functions. Let us define,

$$\xi_k = \epsilon_k - \mu \tag{A.3}$$

The average occupation corresponds, obviously, to the Fermi-Dirac distribution,

$$\langle n_k \rangle = \frac{1}{\mathrm{e}^{\beta(\xi_k)} + 1}. \tag{A.4}$$

The average energy is given by,

$$\langle E_k \rangle = (\epsilon_k - \mu) \langle n_k \rangle \tag{A.5}$$

The specific heat is given by,

$$c_V^k = \frac{k_B \xi_k^2}{4 \cosh(\xi_k/2)} \tag{A.6}$$

The specific heat is therefore even in ξ_k, i.e,

$$c_v^k(\varepsilon_k - \mu) = c_v^k(\mu - \varepsilon_k) \tag{A.7}$$

For finite temperature and finite chemical potential,

$$c_v^k \sim \begin{cases} \mathrm{e}^{\beta(\xi_k)}, & \xi_k \ll 0 \\ \left(\frac{\beta}{2}\right)^2 (\xi_k)^2, & \xi_k \approx 0 \\ \mathrm{e}^{-\beta(\xi_k)}, & \xi_k \gg 0 \end{cases} \tag{A.8}$$

Therefore the chemical potential is zero for $\epsilon_k = \mu$, behaves quadratically around this point, with the concavity of the parabola controlled by the temperature, and falls exponentially to zero for $|\epsilon - \mu| \gg 0$. The specific heat as a function of ϵ_k, is plotted in Fig. A.2 for several temperatures.

[1] We have neglected spin since the situation with spin is pretty much the same.

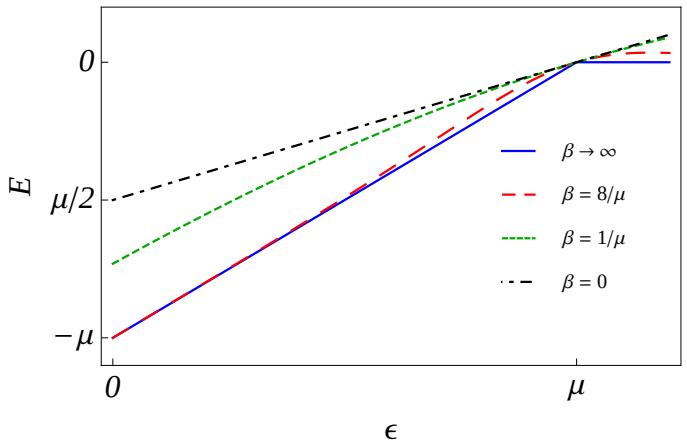

Figure A.1: Fermionic oscillator average energy as a function of the single particle energy.

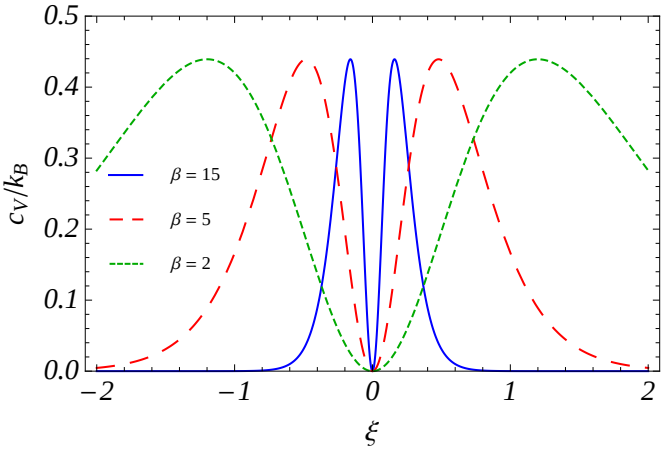

Figure A.2: Fermionic oscillator specific heat as a function of the single particle energy.

Bibliography

[1] A. Geim. Many Pioneers in Graphene Discovery. *APS News*, 19(1):4, 2010.

[2] K. S. Novoselov, A. K. Geim, S. V. Morozov, D. Jiang, Y. Zhang, S. V. Dubonos, I. V. Grigorieva, and A. A. Firsov. Electric Field Effect in Atomically Thin Carbon Films. *Science*, 306(5696):666–669, 2004.

[3] K. I. Bolotin, K. J. Sikes, Z. Jiang, M. Klima, G. Fudenberg, J. Hone, P. Kim, and H. L. Stormer. Ultrahigh electron mobility in suspended graphene. *PNAS*, pages 1–5, 2008.

[4] K. S. Novoselov, Z. Jiang, Y. Zhang, S. V. Morozov, H. L. Stormer, U. Zeitler, J. C. Maan, G. S. Boebinger, P. Kim, and A. K. Geim. Room-Temperature Quantum Hall Effect in Graphene. *Physica E*, 293(2000):84173–84173, 2005.

[5] R. E. Peierls. Quelques proprietes typiques des corpses solides. *Ann. I. H. Poicare*, 5(3):177–222, 1935.

[6] L. D. Landau. Zur Theorie der phasenumwandlungen II. *Phys. Z. Sowjetunion*, 11:26–35, 1937.

[7] N. W. Ashcroft and N. D. Mermin. *Solid state physics*. Thomson Learning.

[8] W. Ehrenberg and R. E. Siday. The Refractive Index in Electron Optics and the Principles of Dynamics. *Proceedings of the Physical Society. Section B*, 62(1):8–21, January 1949.

[9] Y. Aharonov and D. Bohm. Significance of Electromagnetic Potentials in the Quantum Theory. *Physical Review*, 115(3):485–491, August 1959.

[10] R. Montenegro-Filho and M. Coutinho-Filho. Doped AB2 Hubbard chain: Spiral, Nagaoka and resonating-valence-bond states, phase separation, and Luttinger-liquid behavior. *Physical Review B*, 74(12):1–10, 2006.

[11] A. Macêdo, M. dos Santos, M. Coutinho-Filho, and C. Macêdo. Magnetism and Phase Separation in Polymeric Hubbard Chains. *Physical Review Letters*, 74(10):1851–1854, March 1995.

[12] Y. Duan and K. Yao. Theoretical model of an organic ferrimagnetic state for a bipartite lozenge chain. *Physical Review B*, 63(13), March 2001.

[13] Z. Gulácsi, A. Kampf, and D. Vollhardt. Exact Many-Electron Ground States on the Diamond Hubbard Chain. *Physical Review Letters*, 99(2):2–5, 2007.

[14] Jerome Silvestre and Roald Hoffmann. Tetrahedral and square-planar one-dimensional chains: the interplay of crystal field and band width in MS2 compounds. *Inorganic Chemistry*, 24(24):4108–4119, November 1985.

[15] H. Kikuchi, Y. Fujii, M. Chiba, S. Mitsudo, T. Idehara, T. Tonegawa, K. Okamoto, T. Sakai, T. Kuwai, and H. Ohta. Experimental Observation of the 1/3 Magnetization Plateau in the Diamond-Chain Compound Cu3(CO3)2(OH)2. *Physical Review Letters*, 94(22), June 2005.

[16] M. Büttiker, Y. Imry, and R. Landauer. Josephson behavior in small normal one-dimensional rings. *Physics Letters A*, 96(7):365–367, July 1983.

[17] A. A. Lopes. *The Aharonov-Bohm effect and persistent currents in quantum rings*. Bsc thesis, University of Aveiro, 2008.

[18] A. Castro Neto, F. Guinea, N. Peres, K. Novoselov, and A. Geim. The electronic properties of graphene. *Reviews of Modern Physics*, 81(1):109–162, January 2009.

[19] E. H. Lieb. The Hubbard model: some rigorous results and open problems. pages 1–20, 1993.

[20] H. Tasaki. From Nagaoka's Ferromagnetism to Flat-Band Ferromagnetism and Beyond. *Progress of Theoretical Physics*, 99(4):489–548, April 1998.

[21] E. Jagla and C. Balseiro. Electron-electron correlations and the Aharonov-Bohm effect in mesoscopic rings. *Physical Review Letters*, 70(5):639–642, February 1993.

[22] J. Rincón, A. A. Aligia, and K. Hallberg. Features of spin-charge separation in the equilibrium conductance through finite rings. *Physical Review B*, 79(3):1–7, January 2009.